

1 *Review*

2 Protein and Polysaccharide-Based Fiber Materials 3 Generated from Ionic Liquids: A Review

4 Christopher R. Gough ^{1,2}, Ashley Rivera-Galletti ^{1,2}, Darrel A. Cowan ^{1,2}, David Salas-de la Cruz ³,
5 Xiao Hu ^{1,4,5*}

6 ¹ Department of Physics and Astronomy, Rowan University, Glassboro, NJ 08028, USA

7 ² Department of Chemistry and Biochemistry, Rowan University, Glassboro, NJ 08028, USA

8 ³ Department of Chemistry, and Center for Computational and Integrative Biology, Camden, NJ 08102, USA

9 ⁴ Department of Biomedical Engineering, Rowan University, Glassboro, NJ 08028, USA

10 ⁵ Department of Molecular and Cellular Biosciences, Rowan University, Glassboro, NJ 08028, USA

11 * Correspondence: hu@rowan.edu; Tel.: +1-856-256-4860, Fax: +1-856-256-4478

12 Received: date; Accepted: date; Published: date

13 **Abstract:** Natural biomacromolecules such as structural proteins and polysaccharides are composed
14 of the basic building blocks of life: amino acids and carbohydrates. Understanding their molecular
15 structure, self-assembly and interaction in solvents such as ionic liquids (ILs) is critical for
16 unleashing a flora of new materials, revolutionizing the way we fabricate multi-structural and
17 multi-functional systems with tunable physicochemical properties. Ionic liquids are superior to
18 organic solvents because they do not produce unwanted by-products and are considered green
19 substitutes because of their reusability. In addition, it will significantly improve the miscibility of
20 biopolymers with other materials while maintaining the mechanical properties of the biopolymer
21 in the final product. Understanding and controlling the physicochemical properties of biopolymers
22 in ionic liquids matrices will be crucial for progress leading to the ability to fabricate robust multi-
23 level structural 1D fiber materials. It will also help to predict the relationship between fiber
24 conformation and protein secondary structures or carbohydrate crystallinity, thus creating potential
25 applications for cell growth signaling, ionic conductivity, liquid diffusion, thermal conductivity,
26 and several applications in biomedicine and environmental science. This will also enable the
27 regeneration of biopolymer composite fiber materials with useful functionalities and customizable
28 options critical for additive manufacturing. The specific capabilities of these fiber materials have
29 been shown to vary based on their fabrication methods including electrospinning and post-
30 treatments. This review serves to provide basic knowledge of these commonly utilized protein and
31 polysaccharide biopolymers and their fiber fabrication methods from various ionic liquids, as well
32 as the effect of post treatments on these fiber materials and their applications in biomedical and
33 pharmaceutical research, wound healing, environmental filters, sustainable and green chemistry
34 research.

35 **Keywords:** Protein; Polysaccharides; Fibers; Biomaterials fabrication; Tissue engineering; Drug
36 delivery; Ionic liquid; Filtration; Green solvents

37

38 1. Introduction

39 Biomaterials derived from natural products have been of interest in recent decades due to their
40 abundance, low cost, biocompatibility, and tunable morphological and physical properties [1-5].
41 These materials have been broadly used for the development of membranes and fibers for liquid and
42 gas separation [6] and sensing [7, 8], fabrication of tissue engineering scaffolds for neural [9] or bone
43 regeneration [10], and for the fabrication of nanostructures for drug delivery [11]. The study of

44 biomaterials includes aspects of medicine, biology, chemistry, engineering, environmental science,
45 and materials science. These materials are extremely versatile as shown from a variety of biopolymers
46 used in nature, such as in spider silk which has the overall highest tensile strength in nature while
47 maintaining a very high elasticity, and chitin that is used by many insects to provide structural
48 stability and protection. However, to make biopolymers largely available in modern technology,
49 there needs to be the development of new methodologies to tune the properties of these materials to
50 suit specific technological demands.

51 Protein and polysaccharide polymers are composed from the basic building block of life: amino
52 acids and carbohydrates. Understanding the rule of life of these two systems is critical to unleash a
53 flora of new materials that could revolutionize the way we fabricate multi-structural and multi-
54 functional systems. Natural proteins and polysaccharides are relatively inexpensive and easy to
55 process and regenerate, making it an attractive material from an economic perspective. The main
56 advantage of these biopolymer-based materials over synthetic materials in the biomedical field is
57 their unique biodegradability and biocompatibility. Minimizing the host immune response is an
58 important aspect of determining the success of a drug delivery or tissue regeneration operation.
59 Protein and polysaccharide-based biomaterials play a critical role in this process since they can be
60 degraded by natural enzymes in the body, which reduces the accumulation of harmful by-products
61 [12, 13].

62 Solvents are essential, as they are the driving force for the dissolution of the protein and the
63 polysaccharide. A poor solvent will significantly affect the miscibility of protein or polysaccharide
64 polymers and reduce the mechanical properties of the final materials [14-16]. In addition, many
65 organic solvents will markedly alter the original molecular weight of protein materials such as silks
66 [17]. Therefore, the use of ionic liquid (IL) is frequently applied for tuning the final properties of the
67 material. Ionic liquids have been used to dissolve both polysaccharides and selected proteins such as
68 silk, keratin, and collagen without changing their molecular weights [18-20]. They have an advantage
69 over organic solvents as they do not lead to unwanted side products and are considered as a green
70 alternative as they encompass the ability to be reusable [21]. The composition of an ionic liquid is
71 very important as it combines a bulky asymmetric cation with a weakly coordinated anion, which
72 can cause changes in the intra- and inter-molecular interactions [22-25]. When biopolymers are
73 dissolved in ionic liquids, the anion forms hydrogen bonds with hydroxyl groups in the biopolymer,
74 disrupting the naturally occurring hydrogen bonding network while the cation associates with the
75 ether oxygen atoms and CH groups [26], thus causing a change in the molecular conformation. To
76 improve interactions of a biopolymer material, such as silk or keratin between itself or other
77 materials, one can increase interfacial adhesion while mitigating interfacial tension of the material.
78 This can be accomplished by dissolving the biomacromolecules and reforming them in a solvent, via
79 a coagulation process, to promote stabilization and formation of secondary structures embedded in
80 a matrix by hydrogen bonds, electrostatic interactions, and covalent bonds [23, 24, 26]. In addition,
81 the coagulation solvent could act as a nucleating agent to increase the nucleation and overall
82 crystallization rate leading to changes in the natural conformation of the biopolymers [27].
83 Controlling the formation of protein secondary structures and polysaccharide crystallites are crucial
84 for these studies.

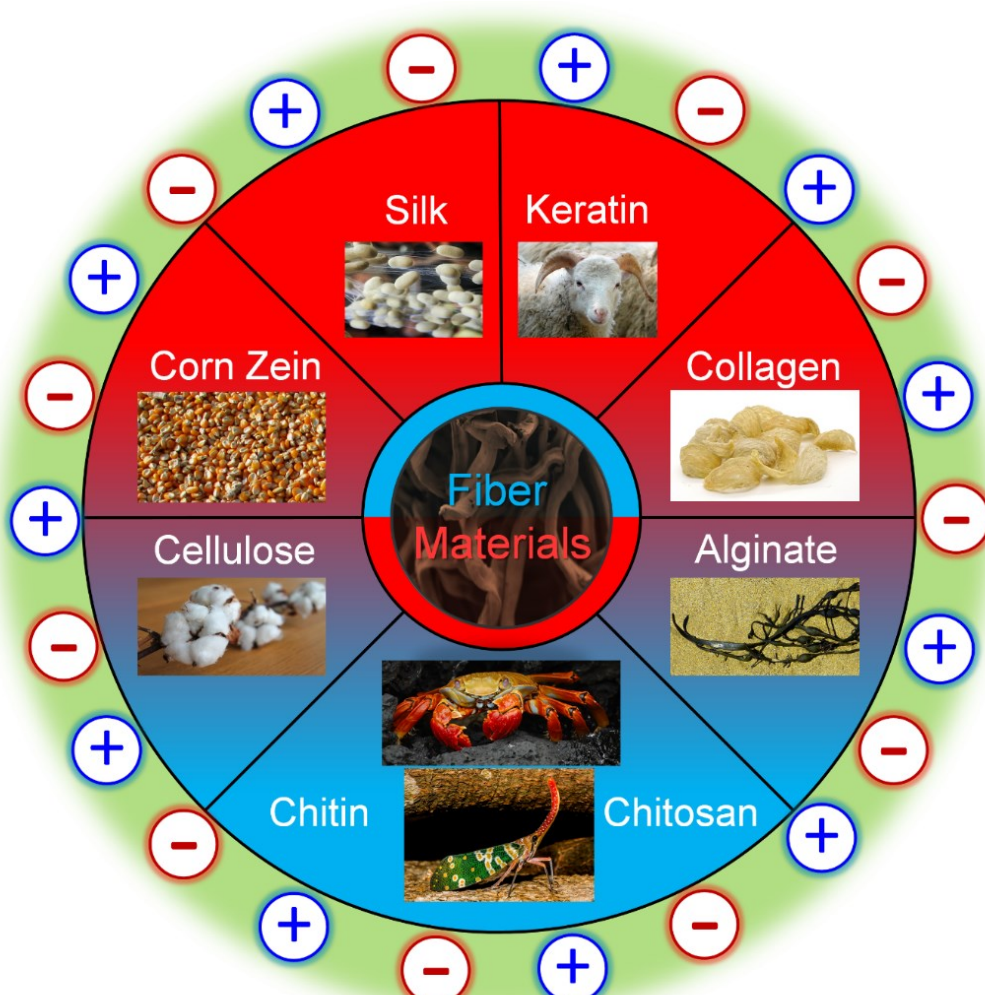
85 The use of fibrous materials in biomedical research is becoming increasingly popular due to their
86 high surface-area-to-volume ratio, mechanical strength, porosity, and tunability. Fibers made from
87 natural biopolymers are biodegradable and biocompatible and therefore enzymes in the body can
88 degrade these fibers into nontoxic metabolites that can be reabsorbed. The incorporation of natural
89 biopolymers into biological materials has also been shown to enhance cell attachment due to the
90 presence of native cell attachment motifs and increases cell migration and proliferation [28, 29].
91 Therefore, the use of biopolymer-based fibers in tissue engineering and nanomedicine has medical
92 and commercial appeal. However, despite these advantages, the improvement of the mechanical and
93 physical properties of biopolymer-based fibers remains challenging. Thus, biopolymer-based fibrous
94 materials can be further modified by crosslinking or blending with other biocompatible materials to

95 form a tunable platform. These characteristics are also highly dependable on the type of
96 manufacturing method used to make the fibers.

97 This review provides a basic knowledge of the commonly used materials and methods for the
98 fabrication of protein or polysaccharide-based fibers through various ionic liquids, as well as their
99 corresponding use in tissue engineering, water filtration, and drug delivery. Popular proteins and
100 polysaccharides such as keratin, collagen, silk, elastin, corn zein, soy, cellulose, and chitin are of
101 particular interest. Electrospinning is currently the most popular fabrication technique, with several
102 modifications also used, such as wet/dry jet spinning. Protein and polysaccharide materials have also
103 been shown to vary depending on the solvent used (ionic liquid type or other organic solvents), the
104 fiber post treatment (such as various coagulation agents), as well as the composition of the fiber. In
105 addition, this review article will discuss the current understanding of interactions between natural
106 polysaccharides and structural proteins through their composite materials, which directly affect the
107 morphology and physical, thermal and mechanical properties of the matrix in ionic liquids, such as
108 the material crystallite formation and protein secondary structure in the 1D fibers.

109 2. Typical Biopolymers from Proteins and Polysaccharides

110 Several distinct kinds of proteins and polysaccharides are used in present-day research,
111 including composite mixtures of both. Some commonly used materials are listed below in **Figure 1**
112 with their sources. Depending on the desired application and properties of the material being made,
113 however, other proteins and polysaccharides can be used. The main difference between proteins and
114 polysaccharides is that proteins are composed of amino acids, while polysaccharides are composed
115 of long chains of sugar molecules. On a smaller scale, proteins are synthesized from long chains of
116 peptides to form their primary structure. From there, various interactions with itself or other proteins
117 including hydrogen and disulfide bonding, London Dispersion forces, and charge-charge
118 interactions allow proteins to form higher-order structures including coils, helices, and sheets.
119 Polysaccharide chains tend to be more limited in their interactions, which limits their higher order
120 structures. Nonetheless, polysaccharides are long chains of sugar monomers that interact with each
121 other and other polysaccharides through glycosidic linkages and hydrogen bonding to form
122 polymers of long chains. In addition, many hybrid materials are made that combine proteins and
123 polysaccharides together.



124

125

Figure 1. Commonly used protein and polysaccharide fiber materials that can be generated from ionic liquids with anions and cations and their natural sources. Protein materials are in red, while polysaccharides are in blue.

126

2.1. Protein materials

127

2.1.1. Silk proteins

128

Silk protein, generally, is a fibrous material that is spun by a variety of arthropod species. These fibers are semicrystalline with an ordered structure within a nebulous matrix [30]. Five different structures have been identified in silk proteins with vastly different molecular organization including coiled coil, extended beta sheet, cross-beta sheet, collagen-like triple helix, and polyglycine II [31-33]. These unique structures require specific amino acid sequences in the proteins, and each provide unique material properties to the protein. This means different silk proteins vary in their mechanical strength, thermal properties, bioactivity, chemical activity, and how well they blend into composites with other proteins. Because of this, silk has been used as thin protein films [29, 34, 35] and nanofibers [36-38] in a wide variety of applications including delivery of drugs [39] and cytokines [40], tissue engineering [38, 41, 42] and textile electronics [43-45]. Silk has been used in the textile industry for hundreds of years and is mechanically strong. The ability to tune its mechanical properties by varying the beta sheet content makes silk a widely used biomaterial today. Plentiful literature has shown the ability of silk to dissolve in ionic liquids, including for the formation of fiber materials [18, 46-49].

129

2.1.2. Keratin proteins

144 Keratin is another naturally-derived protein being used for biomedical and bioelectronic
145 purposes. Keratin is often extracted from wool fibers and processed into nanofibers [50, 51]. Other
146 sources of keratin include feathers, hair fibers, fingernails, and horns. Depending on the source,
147 different forms of keratin can be extracted. α -keratin, for example, creates fibrils made up of
148 intermediate filaments. Although keratin is mechanically weaker than silk, studies have been
149 conducted to try to improve its mechanical strength [52]. Like other biomaterials, keratin is often used
150 for its high biocompatibility and strong material properties. The applications of keratin include tissue
151 engineering [53, 54], drug delivery [55], and food packaging [56]. Several different types of keratin
152 exist in nature, due to an abundance of amino acid substitutions that occur in the molecule. For
153 example, keratin 14 is a structural protein found in basal cells in the epithelium when paired to
154 keratin 5; when the methionine amino acid in keratin 14, a hydrophobic, nonpolar amino acid, is
155 substituted with threonine, a hydrophilic, polar amino acid, a severe skin disease is developed [57].
156 Other mutations can also cause less severe diseases, such as substituting methionine to arginine in
157 the linker region of the keratin. The unique amino acids in keratin also serve a strong purpose in
158 packaging; the high amount of polar amino acids in natural keratin sources allows for membranes
159 with high adsorption for Cu(II) and other metals [50]. Because of the strong outer cuticle in keratin
160 fibers due to heavy crosslinking with disulphide bonds, many common solvents are unable to
161 dissolve it. Ionic liquids, however, show potential as a solvent for dissolving keratin due to the ability
162 of select ILs to disrupt disulphide bonds [58, 59]. This ability gives ILs strong potential in keratin fiber
163 formation.

164 2.1.3. Soy proteins

165 Another attractive protein for material applications is soy extracts. Soy proteins are globular
166 proteins consisting of two main units conglycinin 7S and glycinin 11S. Both of these units are
167 primarily dominated by a random coil structure and contain subproteins of varying molecular
168 weights. They can be either water-soluble albumins or globulins soluble in salt solutions, with the
169 majority of soy proteins being the latter [60]. Isolates from soy protein contain several functional
170 groups that can interact with the surrounding environment, making them useful for several
171 applications like pollutant filtering [61], adhesives [60], and inhibiting oxidation [62]. In general
172 applications, soy proteins are often used in tissue engineering [63, 64] and have been used to create
173 microcapsules [65]. Since soy proteins and isolates from soy proteins lack the mechanical integrity of
174 other proteins, researchers often create composites with more mechanically stable polymers in order
175 to create strong biomaterials with the application potential of soy. Because of this, the cosolvent
176 potential of ILs is highly appealing and widely studied [66, 67].

177 2.1.4. Collagen

178 Collagen can assemble into 29 different types, each with its own type distribution and signaling
179 abilities *in vivo* [68], but the majority of collagen in the body is either collagen I, II, or III. Collagen's
180 repeating amino acid sequence allows it to form a stable secondary protein structure consisting of
181 triple helices. These helices can further assemble into quaternary structures, which allows collagen to
182 assemble into fibrillar proteins found throughout the body and in collagen V and XI. Upon
183 dissolution in IL, the triple helical structure of collagen can be partially destroyed, but still regenerate
184 into fiber [69]. Additionally, collagen is dissolvable in several types of IL [70] with both stabilizing or
185 destabilizing effects depending on the ionic effects of the IL [71].

186 Nanofibers, protein films, and hydrogels are all commonly used forms of collagen in material
187 engineering. Type I collagen is the most widely used form of collagen as a biomaterial due to its
188 abundance in nature. It also allows for successful mimicry of human extracellular matrix (ECM), since
189 collagen I is a major component of it.

190 2.1.5. Elastin

191 Elastin is a vital protein found in the ECM of the body in order to provide elasticity and resiliency
192 to tissues and organs. Where collagen provides structure and strength to the body, elastin provides
193 flexibility. Elastin is primarily found in the lungs, aorta, and skin where elasticity is crucial [72].
194 During fiber formation, elastin molecules bind to other ECM proteins and uncoil into elongated
195 chains which are able to crosslink with each other by oxidizing lysine residues [73]. Due to its
196 elasticity and origins near the ECM, elastin is a popular biomaterial choice for vascular tissue
197 engineering and other materials that need to interface with blood [74]. Elastin is also frequently used
198 a skin substitute to treat burns and chronic wounds due to its importance in native skin tissue,
199 however the actual elastin content is low in these scaffolds [75]. Elastin scaffolds must be combined
200 with a mechanically stronger material such as collagen. Self-assembling proteins is a popular topic in
201 current research and is an area where elastin receives frequent attention. Currently, there is literature
202 on elastin's ability to self-assemble in fibers, hydrogels [76], sheets [77], nanoparticles [78], sponges
203 [79], and nanoporous materials [80]. Although elastin is difficult to dissolve, IL can be used to
204 separate it from biomass [81].

205 2.1.6. Corn Zein

206 Zein is a major storage protein of corn, making it a very abundant source for biomaterials and it
207 is also easily extracted. As a coproduct of the bioethanol industry, zein is abundant. Corn zein comes
208 in several different forms. As a nanofiber they tend to show a random coil protein structure and as a
209 thin film they tend to show a more alpha-helical protein structure. It is widely used as a biomaterial
210 due to its abundance and ease to extract, while maintaining good biocompatibility. In current
211 research, zein is frequently used in tissue engineering [82, 83] and drug delivery [84]. Zein can also
212 be chemically modified in order to improve its mechanical properties [85]. IL have proven to be an
213 effective solvent for zein proteins, obtaining a concentration of up to 10% w/w in BMIMCl and
214 BMIMdca or up to 15% wt% in C₄C₁ImCl [86]. The highest concentrations found in literature were 70
215 wt% from protic ILs NH₃(CH₂CH₂OH)OFO and NH₃(CH₂CH₂OH)OAc [87], although this produced
216 impractical, viscous solutions. In the same study, more practical solutions of 20 wt% were produced
217 with conventional heating at 120°C or using a microwave.

218 2.1.7. Reflectin

219 A relatively new class of proteins, first reported in 2004, is the reflectin protein. These proteins
220 are given their name from their unique spectral and optical properties, which allow them to self-
221 assemble into reflecting materials [88]. In nature, reflectin proteins have been identified in
222 cephalopods and in squids, where both animals use reflectin's optical properties for camouflage. The
223 dynamic structural colors caused by this protein are reported to be due to hierarchical assembly on
224 the nanoscale assembly level [89]. Better understanding of this assembly could lead to the design of
225 biomaterials with complex optical functions such as contact lenses. Recently, reflectin was used for a
226 neural stem cell scaffold in order to promote human neural stem/progenitor cell function [90]. Being
227 a new material, the solubility of reflectin in IL has not directly been studied; however reflectin has
228 been dissolved in organic solvents with the intent to process into fibers [91]. Research has shown that
229 "osmotic motors" control the refractive index of reflectin proteins, with positively charged linker
230 segments that are restricted by Coulombic repulsion [92]. ILs, then, could potentially use ionic
231 interactions to tune the refractive properties of reflectin for specific applications. By neutralizing the
232 linker segments in reflectin, these linker segments are able to overcome Coulombic repulsion and re-
233 assemble into multimeric spheres of well-defined size and dispersity [93]. The wide range of anions
234 available in ILs could result in several different self-assembly positions for reflectin for a wide variety
235 of applications.

236 2.2. Polysaccharide Materials

237 2.2.1. Starch

238 Starch is cited as one of the most promising materials for biodegradable films due to its
239 abundance, low cost, biodegradability, and renewability [94]. The molecular structure of starch is
240 made up of two main structures. Polysaccharide amylose forms linear structures in starch while
241 amylopectin forms branched structures. The amount of each of these varies with the source of the
242 starch, but ranges from 20-25% amylose and 75-80% amylopectin, generally. While amylose is semi-
243 crystalline and soluble in hot water, amylopectin is very crystalline and does not dissolve in water.
244 Chemically, amylose is connected by α -1,4 linked glucose units while amylopectin is branched by
245 short α -1,4 chains linked by α -1,6 bonds [95]. On the macroscale, starch is highly hydrophilic. Because
246 of this, it is disadvantaged in its brittleness, poor elasticity, and poor water resistance. To overcome
247 this, starch is often mixed with fillers that work to minimize these weaknesses. Starch is chemically
248 connected as a series of anhydrous glucose units connected by primarily α -d-(1 \rightarrow 4) glucosidic bonds
249 [95]. ILs have been used to dissolve starch both by itself in concentrations up to 10% w/w [86], and
250 with other biopolymers such as cellulose to form fibers [96].

251 2.2.2. Cellulose

252 Cellulose is one of the most ubiquitous natural polysaccharides. Numerous sources of cellulose
253 exist in nature, including trees, plants, and fruits, due to its important role in the cell wall in plants.
254 Some strains of bacteria are also able to synthesize cellulose. The molecular structure of cellulose
255 consists of repeating glucopyranose molecules covalently linked through acetal functions between
256 hydroxyl groups. It is a linear homopolysaccharide with several hydroxyl groups in the
257 thermodynamically favorable position. During synthesis, cellulose forms microfibrils (2-30 nm
258 diameter) with both crystalline and amorphous regions. Microfibrils will aggregate into bigger fibrils
259 (30-100 nm diameter, 100-500 μ m length) and then into fibers (100-400 nm diameter, 0.5- 4.0 mm
260 length) [97]. Several studies have proven the effectiveness of IL as a solvent for cellulose [98-101] and
261 cellulose composites [48, 49, 102], making it one of the most promising materials for the fabrication
262 of fiber materials using IL as a solvent.

263 2.2.3. Chitin

264 Chitin is the second most abundant natural polysaccharide on earth being found in several
265 sources including crab and shrimp shells, arthropod exoskeletons, and the molluscan shell of squids.
266 Crystals of chitin are referred to as either alpha or beta chitins with most natural sources being the
267 alpha form. Chains of alpha chitin organize themselves antiparallel using intermolecular hydrogen
268 bonds while beta chitin arranges itself in parallel chains. Beta chitin is held together by weaker
269 molecular forces, making it more susceptible to degradation by enzymes or chemical reactions.
270 Gamma chitin is less studied than the other forms, however research into its physicochemical analysis
271 has shown it to be much more like alpha chitin than beta chitin. One significant difference is that
272 gamma chitin organizes itself into microfibers, whereas other forms organize into nanofibers [103].
273 Depending on the source, chitin crystals will form fibrils ranging from 2.5 to 25 nm in length. Unlike
274 most other polysaccharides, which are typically neutral or acidic, chitin is highly basic [104].

275 Chitin's unique optical properties and chelating abilities, combined with its strong mechanical
276 strength and biocompatibility, make it an attractive material for various applications. Common
277 applications include implant devices, wound dressings, drug delivery vehicles, and as a component
278 for systems in regenerative medicine. Chitin fibrils can be converted into nanocrystals, nanofibers,
279 and nanowhiskers via a top-down method and appropriate work-up. A bottom-up approach can also
280 be used to form gels or self-assembled nano-objects can be regenerated from chitin solutions. Chitin's
281 mechanical and chemical stability makes it difficult to dissolve in most common solvents, but ILs
282 have frequently been used to dissolve chitin, including for fiber production [105]. Due to the
283 functionality of chitin and chitosan, chitin fibers have many practical applications including in filters
284 [105] and tissue engineering. Of special importance in using ILs to modify chitin's structure, size, and
285 porosity, is ILs with short substituents a cationic ring [106].

286 2.2.4. Chitosan

287 Chitosan is a deacetylated derivative of chitin. Structurally, chitosan is a linear chain of
288 glucosamine and N-acetyl glucosamine units linked by glycosidic bonds. Chitosan can have varying
289 amounts of glucosamine residues in the polymer chain, which affects the overall properties of the
290 polymer. In order to quantify this, researchers use the degree of deacetylation (DDA), which is the
291 mole fraction of glucosamine residue in the polymer chain [107]. The optimal DDA and molecular
292 weight varies with the intended use of the material, as both of these properties influence the
293 physicochemistry of the molecule including crystallinity, solubility, and degradation [104]. Due to
294 the presence of these amines, as well as primary and secondary alcohol groups, chitosan is a highly
295 practical molecule for functionalization. Similarly to chitin, chitosan is also frequently dissolved
296 using IL to convert it into fibers to expand its application potential [19].

297 2.2.5. Alginate

298 Another source of polysaccharides is alginate. These are produced by bacteria and seaweed and
299 are used in a large variety of applications due to their unique physicochemistry. Of special note here
300 is their use in advanced pharmaceuticals and biomedical applications within the last couple of
301 decades due to their biocompatibility, nontoxicity, and adept uses. Despite both being classified as
302 alginate, bacteria and seaweed alginate have several differences in composition, modifications,
303 molecular mass, viscoelasticity, and polydispersity [108]. Molecularly, alginate is a linear,
304 nonbranching polysaccharide consisting of two types of uronic acid residues linked by glycosidic
305 bonds [108]. In nature, alginates usually have a heteropolymeric combination of residues with a
306 varying occurrences of β -D-mannuronic acid (M) residues and epimer α -L-guluronic acid (G)
307 residues. Recent research, however, has been able to produce monopolymers using
308 genetically mutated *P. aeruginosa* bacteria [109, 110]. An important note with bacteria-made alginate
309 is that they can be subject to post-translational modifications that cause significant structural changes;
310 bacteria can also naturally acetylate alginates at the O-2 and/or O-3 positions [110]. The resulting
311 composition affects the overall physicochemistry properties of the alginate including viscoelasticity,
312 crosslinking ability [111], strength, stability, and mechanical properties [111-114], solubility, water
313 capacity, and molecular mass [109, 115-117]. These unique qualities lead to a wide range of
314 applications including alginate's use in nanoparticles, nanotubes, microspheres, microcapsules,
315 sponges, hydrogels, foams, elastomers, and fibers [118-128]. Recently, IL has been used to dissolve
316 alginates with other biopolymers to form stable biomaterials [129, 130].

317 2.3. Protein and polysaccharide based composite materials

318 In biological systems, most structural materials are composites formed from a dispersed phase,
319 typically biomacromolecules arranged in a hierarchically assemblage. For example, in wood,
320 cellulose is in the dispersed phase, and interacts within a matrix composed of other polysaccharides
321 such as xylan and lignin. In another example, the exoskeleton of arthropods, chitin, another
322 polysaccharide, is in the dispersed phase within a matrix of silk-like proteins. Recent reports
323 characterizing the fabrication of biomaterial composites (biocomposites) using natural materials such
324 as silk, cellulose, bacterial cellulose, and chitosan have identified changes in physicochemical and
325 morphological properties as a function of fabrication method and material composition [131-133].
326 However, the relationship between hierarchical and secondary structures during materials formation
327 is important but still astonishingly unclear. An important obstacle in the fabrication of biocomposites
328 is an inability to predict the relationship between the complex hierarchical structure and the
329 physicochemical properties of a biomaterial. The ability to manipulate molecules to form hierarchical
330 structures with precise control, size, spacing, and shape is a central requirement for achieving the
331 goal of the rapid fabrication of multi-level structures from single structures. In some protein-
332 polysaccharides composites, beta-sheet crystallites provide crosslinks and enhanced mechanical
333 properties. However, their morphology is dependent on preparation conditions and material
334 composition. Currently, the means to control the development of characteristics such as crystallite

size and shape are still lacking. Achieving this level of understanding and control will be crucial for progress leading to the ability to fabricate robust multi-level structural biocomposites such as micro-/nano-fibers. Understanding molecular self-assembly behaviors and spatiotemporal morphologies in multi-level structural biocomposites will be essential to defining and characterizing the basic phenomena and mechanisms that control morphology and physicochemical properties and finally the materials usability.

3. Fabrication Methods to Control Fiber Formation

3.1. Solvents useful for biopolymer dissolution

3.1.1. Ionic liquids as solvents

Ionic liquids, traditionally known as room temperature ionic liquids (RTILs), are molten salts that have a melting temperature below 100 °C [134]. Ionic liquids have a wide range of uses in organic synthesis, because they can serve as solvent for many substances, including recalcitrant biopolymers such as cellulose. RTILs have this property because they are made up of polar organic and inorganic components. They have an evaporation temperature greater than 127 °C, and a density greater than that of water. Additionally, they are known as green solvents, meaning that they are able to be regenerated and reused multiple times [135].

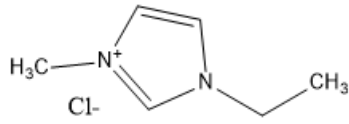
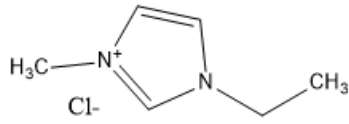
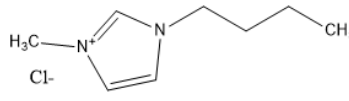
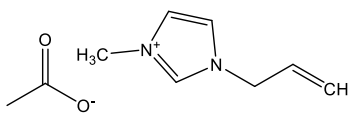
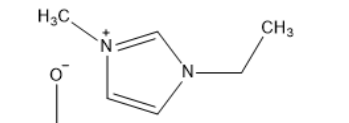
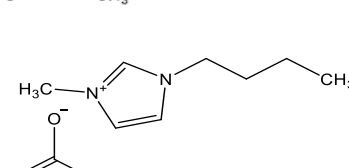
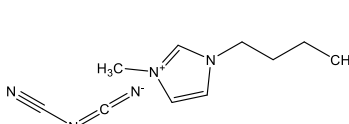
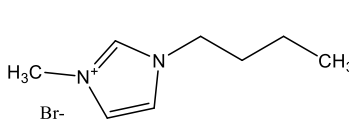
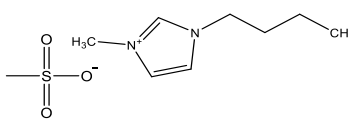
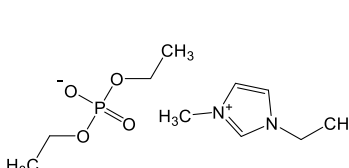
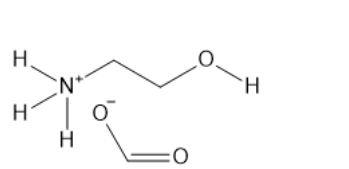
Ionic liquids are ideal solvents for the dissolution of polysaccharides and protein and are commonly used in biopolymer synthesis. Studies have shown that imidazolium derivates are able to blend different proteins and polysaccharides together to create biomaterials, such as biofilms and biofibers. It does this by dissolving both components, denaturing the secondary structure, and creating intermolecular interactions without changing the molecular weight or the primary structure. In comparison to traditional organic solvents, Wang et al. demonstrated that ionic liquids successfully dissolve both polysaccharides and protein without altering the molecular weight [49]. Of particular interest are ionic liquids that have been used to blend together silk and cellulose. Frequently used ILs are 1-allyl-3-methylimidazolium chloride (AMIMCl), 1-butyl-3-methylimidazolium chloride (BMIMCl), 1-Ethyl-3-methylimidazolium chloride (EMIMCl), 1-allyl-3-methylimidazolium acetate (AMIMAc), 1-butyl-3-methylimidazolium acetate (BMIMAc), and 1-Ethyl-3-methylimidazolium acetate (EMIMAc). **Table 1** provided a legend of ionic liquid names, abbreviations and chemical structures commonly used for biopolymer study.

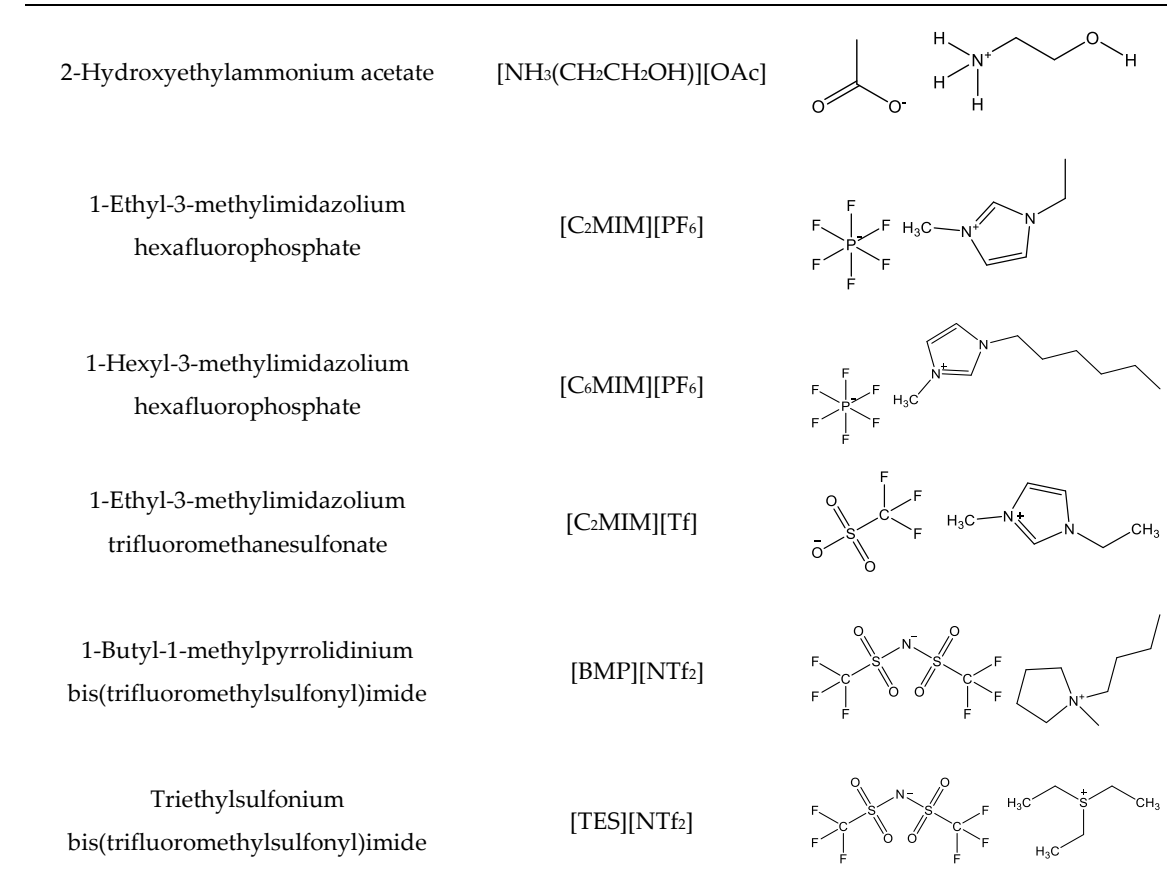
Figure 2 illustrates the cations and anions of these ionic liquids. Each ionic liquid contains an imidazolium cation that has a variable hydrocarbon side chain. Anions found in ionic liquids are mostly monatomic excluding organic and inorganic polyatomic ions such as acetate, sulfonate, and hexafluorophosphate. Each cation combines with the anion to form an ionic bond [136].

Another advantage of using ionic liquids to dissolve and blend proteins and polysaccharides is that they can be washed from the blend using a polar solvent and regenerated for reuse in subsequent experiments. The most commonly used solvents are distilled/deionized water, ethanol, and hydrogen peroxide [136]. The liquids can be separated via simple evaporation/distillation because of the apparent differences in boiling points of the two liquids. This makes the regeneration process relatively inexpensive and sustainable. The variations in the structure of ionic liquids can be used to control the physio-chemical properties of the subsequent created nanoparticles.

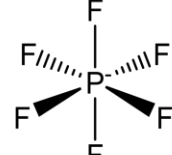
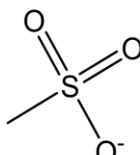
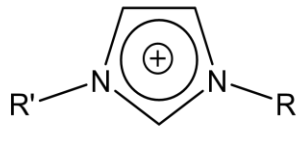
Table 1. Ionic liquid names, abbreviations and chemical structures commonly used for biopolymer study.

Ionic Liquid	Abbreviation(s)	Chemical Structure
1-Allyl-3-methylimidazolium chloride	AMIMCl	

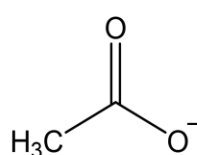
	[C ₂ MIM][Cl]	
1-Ethyl-3-methylimidazolium chloride	or EMIMCl	
1-Butyl-3-methylimidazolium chloride	[C ₄ C ₁ IM]Cl or BMIMCl	
1-Allyl-3-methylimidazolium acetate	AMIMAc	
1-Ethyl-3-methylimidazolium acetate	[C ₂ MIM][CH ₃ CO ₂] or [C ₂ MIM][OAc] or EMIMAc	
1-Butyl-3-methylimidazolium acetate	BMIMAc	
1-Butyl-3-methylimidazolium dicyanamide	[BMIM][DCA]	
1-Butyl-3-methylimidazolium bromide	BMIMBr	
1-Butyl-3-methylimidazolium methanesulfonate	BMIMMeSO ₃	
1-Ethyl-3-methylimidazolium diethyl phosphate	EMIMDep	
2-Hydroxyethylammonium formate	[NH ₃ (CH ₂ CH ₂ OH)][OFO]	



377

Imidazolium Cations:**Typical Anions:**Methanesulfonate[MeSO₃⁻]Hexafluorophosphate [PF₆⁻]

examples:

[EMIM]⁺: R'=C₂H₅ and R=CH₃[BMIM]⁺: R'=C₄H₉ and R=CH₃[AMIM]⁺: R'=C₃H₅ and R=CH₃Acetate [OAc⁻]Chloride [Cl⁻]Bromide [Br⁻]

378

379 **Figure 2.** Commonly used ionic liquids for fabricating protein and polysaccharide fiber materials.

380

381 In one study [25], a 10:90 ratio of *B. Mori* silk-cellulose films were investigated as a function of
 382 ionic liquid type. Six types of ionic liquids were used in this study, including AMIMCl, BMIMCl,
 383 EMIMCl, EMIMAc, 1-Butyl-3-methylimidazolium bromide (BMIMBr), and 1-Butyl-3-
 384 methylimidazolium methane sulfonate (BMIMMeSO₃). Scanning electron microscope (SEM) images
 385 provided insight into the surface structures of the blended materials: As a function of ionic liquid
 386 type, coagulation carried out in AMIMCl, BMIMCl, or EMIMCl produced uniform structures; The

387 EMIMAc film contained porous regions, whereas, the BMIMBr and the BMIMMeSO₃ films both
388 appeared to have more crystalline morphology. It was also observed that most of morphology
389 changes occurred as a function of anion type in ionic liquids.

390 3.1.2. Other potential solvents

391 Although ionic liquids are quickly becoming the most common solvent for biopolymers, there
392 are several other common solvents that can dissolve recalcitrant organic and biological compounds.
393 In 2005, Kulpinski reported that cellulose nanofibers with diameters of 200–400 nm were produced
394 via electrospinning when N-methylmorpholine-N-oxide (NMMO) was used as a solvent [137].
395 NMMO is a heterocyclic amine oxide and morpholine derivative used in organic chemistry as a co-
396 oxidant. The monohydrate is used as a solvent for cellulose in the Lyocell process to produce cellulose
397 fibers. It dissolves cellulose to form a solution called dope, and the cellulose is reprecipitated in a
398 water bath to produce a fiber [138].

399 Lithium chloride and other alkali solvents have been used to prepare a variety of organic
400 molecules into solution. In particular, lithium chloride (LiCl) and dimethylacetamide (DMA) are
401 known to form an ionic complex that can dissolve the crystalline and amorphous regions of cellulose,
402 chitin, and other polysaccharides [139]. At higher concentrations of LiCl, there is more opportunity
403 for polysaccharides to complex through carbonyl groups or other side chain groups. This allows, in
404 turn, more polysaccharide to be dissolved and then precipitated into a biomaterial.

405 LiCl has also been used in various biomaterial applications of silk. Within tissue engineering,
406 the ability to control a biomaterial's microarchitecture is vital to a successful scaffold implant. In one
407 study, the microarchitecture of silk sericin was precisely controlled using photolithographic
408 fabrication to guide the adhesion of osteoblasts [140], and the solvent used in this study was a mixture
409 of LiCl and dimethyl sulfoxide (DMSO). In a similar study, photolithography was used to pattern
410 thin films with controllable degradation made from silk proteins dissolved in LiCl/DMSO [141]. The
411 same patterning techniques have also been used to create conductive silk biocomposites for
412 degradable bioelectronic sensors [142].

413 Methanoic acid, colloquially known as formic acid, is a common solvent used in the synthesis of
414 biopolymers. The hydrogen ions in formic acid work to interrupt the hydrogen bonds present in the
415 backbone of many organic molecules, disrupting their native structure and allowing the polymer to
416 dissolve into solution. In one study [143], formic acid was shown to dissolve both corn zein and silk
417 fibroin, which can then be spun into nanofibers. Fourier-transform Infrared (FTIR) spectroscopy
418 results show how formic acid was able to modify the protein structure of zein from its native, random
419 coil structure into a more ordered alpha helical structure in its fiber and film forms.

420 In several studies [17, 144], formic acid was mixed with calcium chloride to break down natural
421 silk by disrupting the native structure and breaking down carbon-carbon and carbon-nitrogen chains.
422 Prolonged exposure to formic acid lowered the molecular weight of the silk and affected the thermal
423 stability of the final biopolymer, including its glass transition temperature and region. Similar results
424 could be expected with other natural biopolymers.

425 Aqueous tetrabutylammonium hydroxide (TBAOH) has recently received attention for being an
426 efficient alternative to common organic solvents. In literature, it is commonly used to drive cellulose
427 into solutions with concentrations as high as 10 wt% [145, 146]. At low concentrations (2 wt%),
428 TBAOH is able to dissolve cellulose in minutes at room temperature. Interestingly, this solvent gives
429 some control over the cellulose-cellulose interactions in solution, as cellulose is repulsive in dilute
430 solutions, but attracts into aggregates at concentrations above 0.04 g cm⁻³. In this scenario, cellulose I
431 is soluble, while cellulose II precipitates into aggregates. TBAOH is also a plausible solvent for other
432 biopolymers including silk fibroin in concentrations up to 60 mg mL⁻¹ without adding heat [147].

433 3.2. *Fiber Spinning Methods*

434 3.2.1. Electrospinning

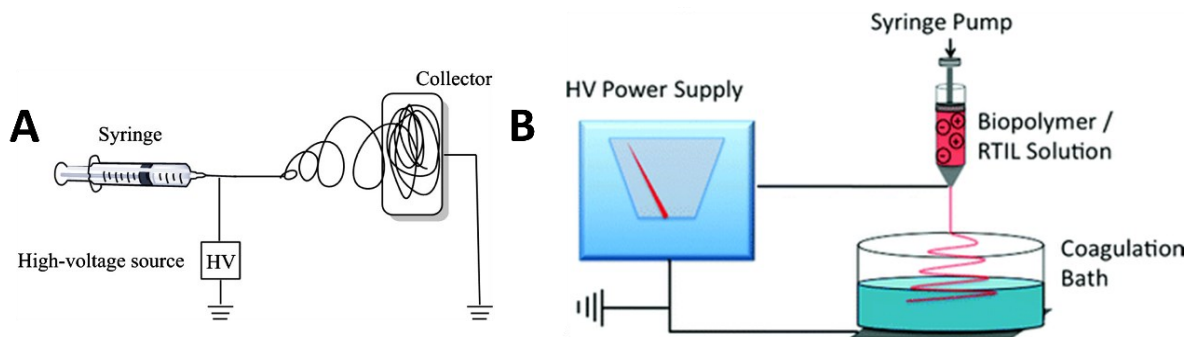
435 Electrospinning is a common method to create micro/nanoscale fibers from biopolymers, which
436 are often difficult to produce, in a simple, cost effective manner [148]. Electrospinning was first
437 patented by Anton Formhals in 1930 [149]. Electrospinning gives unique properties to nanofibers
438 such as large surface area, lower structural defect, and enhanced mechanical properties [150]. Most
439 electrospinning devices are made up of three components: a syringe pump that holds the polymer
440 solution, a high voltage electric source that creates an electrostatic field and draws the solution into
441 a fibrous jet stream, and a grounded target apparatus that collects the nanofibers [136]. The syringe
442 can be attached to a motor that can control and stabilize the rate that the polymer solution is fed to
443 the system. The target apparatus can be modified in several ways to allow for post-production solvent
444 removal or physiological modifications to the fibers.

445 Prior to starting the electrospinning process, the biopolymers are dissolved into a solvent and
446 placed into a syringe. The pump then forces the polymer solution towards the tip of the syringe at a
447 constant rate, where it remains as a drop due to surface tension. The high voltage electrostatic field
448 induces charges in the solution and draws the solution into a Taylor cone. As the charged solution
449 continues to interact with the electric field, the electrostatic forces overcome the surface tension forces
450 and a fiber stream elongates from the stable Taylor cone and travels toward the target apparatus
451 [136]. The stream begins to bend and form large spiral loops as the length increases due to increased
452 instability. The diameter of the loop is inversely proportional to the diameter of the jet but directly
453 proportional to length. Under ideal conditions, the solvent will evaporate as the stream travels to the
454 target site, leaving behind polymer fibers in the range of 10 nm to 10 μ m due to the high surface area
455 to volume ratio. The electrospinning setup can be adjusted to modify the structure of the nanofibers.

456 It is important to note that the appearance of the fibers from the Taylor cone is impacted by
457 several different factors. When the solution initially leaves the cone, it follows a straight path, but it
458 quickly takes on one of three modes based on instabilities in the stream [21]. The instabilities, as
459 described by Shin et al in 2001, are either axis-symmetric, where fluctuations in the fiber stream occur
460 in the central axis, or non-axis-symmetric. The first of the three modes is Rayleigh instability. This
461 mode is produced when the solutions has a high surface tension, and it is suppressed in a high electric
462 field. When the stream exhibits Rayleigh instability, droplets are formed instead of a continuous
463 stream. This is known as electrospraying. The second axis-symmetric mode occurs when the polymer
464 solution is highly viscous leading to the formation of beads in the fiber stream. Lastly, the non-axis-
465 symmetric mode allows for the stream to bend into the ideal spiral loop of nanofibers. This occurs
466 when the solution contains high surface charge density and has a high fluid flow rate. When the
467 stream exhibits non axis-symmetry, the stream will be thinned and smooth nanofibers will be
468 produced [151].

469 The electrospinning setup can play a large role in many of the above-mentioned factors. Because
470 of this, many different variations have evolved from the original horizontal electrospinning setup.
471 **Figure 3** illustrates the basic horizontal electrospinning setup (Fig. 3A) and a wet-spinning setup for
472 IL-based samples (Fig. 3B), where a polymer is electrospun directly into a coagulation agent [21].
473 Other setups include a vertical format of the standard setup, which helps to counter uncooperative
474 electrostatic forces and changes the morphology of the fibers produced [151]. Vertical setups have
475 been further modified by the same author, by utilizing a rotating drum as a collection plate and a
476 rotating disc to further modify the morphology of the fibers produced. Several different
477 modifications of the horizontal electrospinning setup also exist in recent literature: A side-by-side
478 syringe setup is one of these, where, two syringes filled with polymer solution as used
479 simultaneously in order to combine the benefits of two different polymers that may not be compatible
480 with the same solvent [152]. Modifications to the collection plate are also used, such as using parallel
481 plates as a collection target, in order to better control the electrostatic forces that affect polymer
482 trajectory [131]. Another of these modifications builds upon the rotating drum concept by adding a
483 translation element to the drum to further modify fiber morphology [153]. Modifications to the
484 syringe have also been used in recent works, where a process called melt-spinning is used to modify
485 the polymer solution viscosity prior to electrostatic forces taking control [132].

486

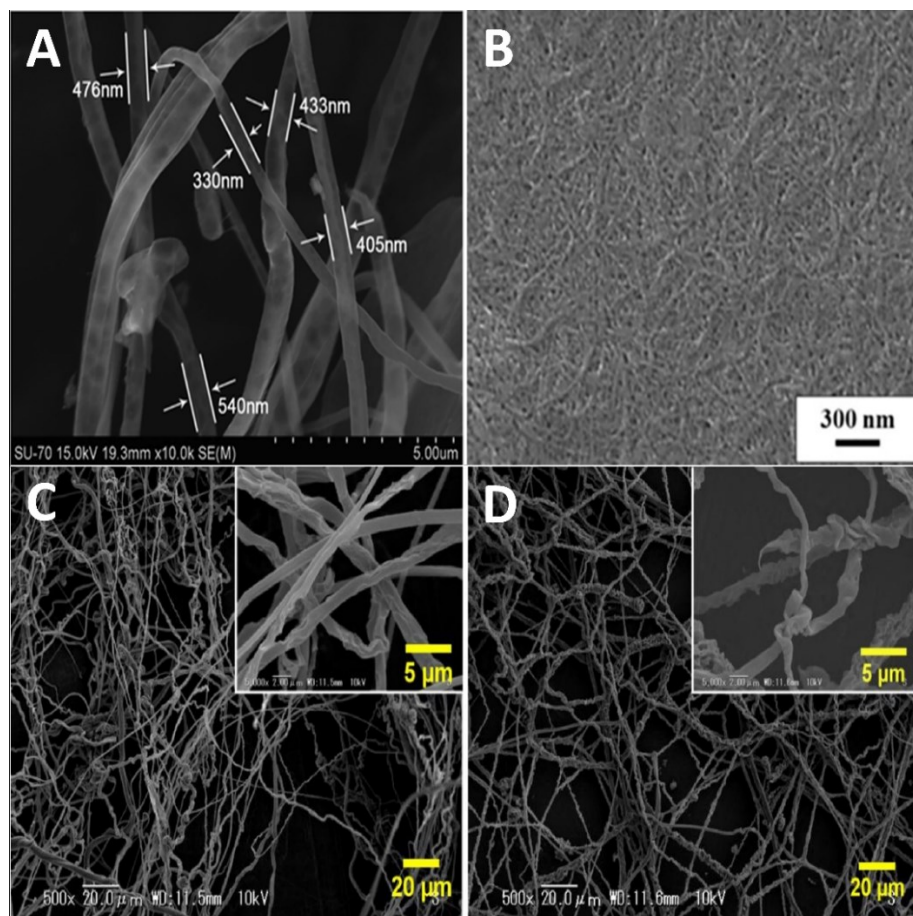


487

488 **Figure 3.** Examples of electrospinning setups utilized with ionic liquid solvents. (A) Basic horizontal
 489 electrospinning setup, with a polymer solution-fed syringe, a high voltage source, and a grounded
 490 collector plate. (B) Wet-spinning where fibers are spun into a coagulation bath instead of a grounded
 491 collection plate. (A is reproduced with permission from Ref. [154]; Copyright 2014 Elsevier. B is
 492 reproduced with permission from Ref. [21]; Copyright 2010 The Royal Society of Chemistry)

493 In addition to solution viscosity, flow rate, surface charge density, and electric field strength, the
 494 spinnability of a biopolymer solution can be controlled by several other parameters related to the
 495 spinning technique and the solution itself. Even the choice of ionic liquid itself can affect the
 496 characteristics of the fibers formed. Critical spinning parameters includes the distance between the
 497 syringe and grounded target, the feed rate, and the electric field strength. The most important
 498 solution parameters are viscosity, surface tension, polymer concentration and molecular weight,
 499 mass distribution, and chemical structure. The last four parameters directly affect chain entanglement
 500 density and spinnability of the polymers [21]. SEM images of a few example nanofibers are shown in
 501 **Figure 4.**

502



503

504 **Figure 4.** SEM images of electrospun nanofibers made from (A) cellulose from [C₂MIM][CH₃CO₂], (B)
505 chitin from[C₂MIM][OAc], and (C) 4.8 wt% and (D) 16.7 wt% cellulose made from [BMIMCl]. (A is
506 used with permission from Ref. [98]; Copyright 2011 The Royal Society of Chemistry. B is used with
507 permission from Ref. [155]; Copyright 2016 European Chemical Societies Publishing. C, D are used
508 with permission from Ref. [99]; Copyright 2018 Elsevier)

509 In the literature, many studies are focused on controlling the physicochemical properties of the
510 nanofibers. One of the most important properties is the diameter of the fiber. Ambient temperature
511 and humidity are two parameters that can affect this property. Pelipenko et al. observed that the
512 diameter of electrospun fibers decreased as the ambient humidity increased [156]. In their
513 experiments, fibers were created from polyvinyl alcohol (PVA) and polyethylene oxide (PEO)
514 polymer solutions as well as PVA/hyaluronic acid (HA) and PEO/chitosan (CS) blended polymer
515 solutions. They observed that diameter of all the nanofibers decreased as the ambient humidity
516 increased. It was also demonstrated that the morphology of the fibers changed as a function relative
517 humidity [156, 157]. As the ambient humidity increased, beads and pores began to develop in the
518 structure of the fibers. In some cases, the increased humidity prevented nanofibers from forming all
519 together and only allowed for electrospraying [158]. This occurs because polymer solutions tend to
520 retain more water when the humidity increases. Increased humidity levels also prevent solvent
521 evaporation as the polymer stream is traveling towards the collector [156].

522 The ambient temperature also affects the diameter of the nanofibers, as reported by De Vrieze et
523 al [156]. In their experiments, nanofibers were electrospun from polyvinylpyrrolidone (PVP) and
524 cellulose acetate (CA) polymer solutions. The PVP was dissolved in ethanol, while CA was dissolved
525 in acetone and dimethylacetamide (DMAC). They observed that the average diameter of the
526 nanofibers spun at 283 K and 303 K was lower than those spun at 293 K, when the relative humidity
527 and the distance between the tip of the syringe and the collector were kept constant. This
528 phenomenon can be explained by two opposing effects: At lower temperatures, the solvent dissolves
529 at a much slower rate. Subsequently, the polymer will need more time to solidify which means the
530 stream will continue to elongate. On the contrary, at higher temperatures, the solution is less viscous
531 which makes it more susceptible to higher stretching and thinning. Bae et al. and Yang et al. reported
532 similar thermal and barometric results in their studies [158, 159].

533 3.2.2. Wet Spinning/Dry-Jet Wet Spinning

534 Wet spinning is a cost-effective fiber fabrication technique that allows for the elongation of a
535 polymer solution in a coagulation bath. In this method, the polymer solution is pumped through a
536 syringe directly into a bath that removes the solvent and allows the polymer to precipitate into a fiber
537 [159]. The fiber can then be elongated by applying tension to the stream and drawing it to the desired
538 length [160]. The setup can be modified to include multiple wash baths and drawing systems to
539 improve molecular alignment and orientation [161].

540 An alternative set up of this technique is call dry-jet wet spinning. In this method, the jet stream
541 is first elongated in air before going into the coagulation bath. This allows for some of the solvent to
542 evaporate, resulting in greater molecular alignment. [162].

543 In contrast to electrospinning, these two techniques do not use an electric field to elongate the
544 fiber stream. This allows for the fibers produced by these methods to have enhanced molecular
545 alignment, but the diameters will be on the micron scale compared to the nanoscale with electrospun
546 fibers [3, 160].

547 3.2.3. Phase Separation

548 Phase separation involves dissolving a polymer system with a solvent and creating a gel from
549 the solution by decreasing the temperature. Once the solution is sufficiently cooled and solidified,
550 the resulting gel can then be soaked in distilled water, which will extract the solvent. Nanofibers will
551 form once the gel is blotted with filter paper and freeze-dried. The structure of the fibers can be

552 controlled by adjusting the concentration of the polymer and the temperature at which the gel is
553 formed [163].

554 **4. Impact of Coagulation and Ions on Material Structure**

555 Once the fibers are produced, several post-treatment steps, including chemical coagulation, can
556 be applied to further enhance or study the morphology and induce ion conductivity of the materials.

557 *4.1. Chemical Coagulation*

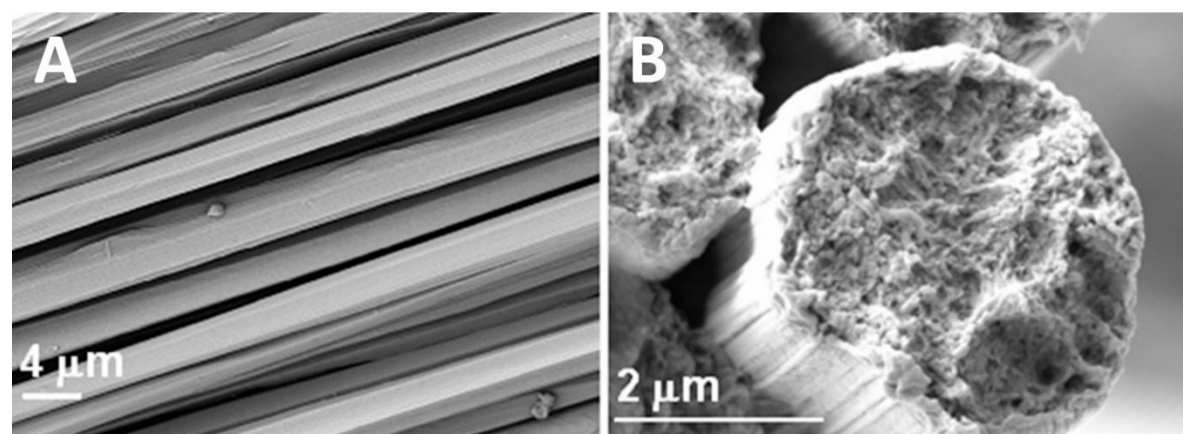
558 Post-production chemical treatments are applied to biopolymer nanofibers to help further
559 extract any remaining ionic liquid from the samples. Removal of the solvent helps to further stabilize
560 and coagulate the nanofiber. Some of the common chemicals used as a wash are water, methanol,
561 and H₂O₂.

562 *4.1.1. Water*

563 Water is an ideal solvent to wash ionic liquids from the surface of the nanofibers. The high
564 polarity of the molecule easily extracts the ionic liquid solvent. When the solvent is removed, the
565 nanofiber will further coagulate and stabilize. This is because the biopolymers are separated due to
566 their electrostatic interactions with the anions in the ionic liquid. The removal of the solvent allows
567 for the biopolymers to interact with each other using hydrogen bonding and causes them to aggregate
568 into a fiber [25]. In addition to ionic liquid extraction, water also helps to modify the diameter and
569 structure of the nanofibers. In 2017, Grimmelsmann et al. reported that the morphology and diameter
570 of chitosan/poly(ethylene oxide) nanofibers was altered after being washed for 30 seconds in
571 deionized water [164]. Even though water is ideal, one disadvantage is that it can replace the ionic
572 liquid and form hydrogen bonds with the biomolecules. This will lead to competition between
573 adjacent biopolymers and water not able to extract any ionic liquid from within the nanofiber. Any
574 solvent trapped within the fiber will be stabilized by the electrostatic attraction to the polymer and
575 protected by the hydrophobic interactions with water. **Figure 5** shows cellulose fibers prepared from
576 cellulose dissolved in ionic liquid and wet-spun directly into a water coagulation bath to form highly
577 crystalline fibers.

578 In another study on *B. Mori* silk-cellulose composites, it showed that water coagulation can
579 change the structure of cellulose microcrystalline, and the β -sheet content of silk can be manipulated
580 by disrupting inter- and intra-molecular hydrogen bonds during the coagulation. The result
581 suggested an intermediate semicrystalline or amorphous structure in the composites, which was
582 confirmed by x-ray scattering [165]. Molecularly, this demonstrated that cellulose microfibril
583 diameter decreased as the silk content increased within the composite of cellulose and silk. As
584 cellulose content increased β -sheets size also increased; even a small percentage of silk (10%) into
585 cellulose caused disruption of the cellulose structure and the assembly into cellulose I structures.

586



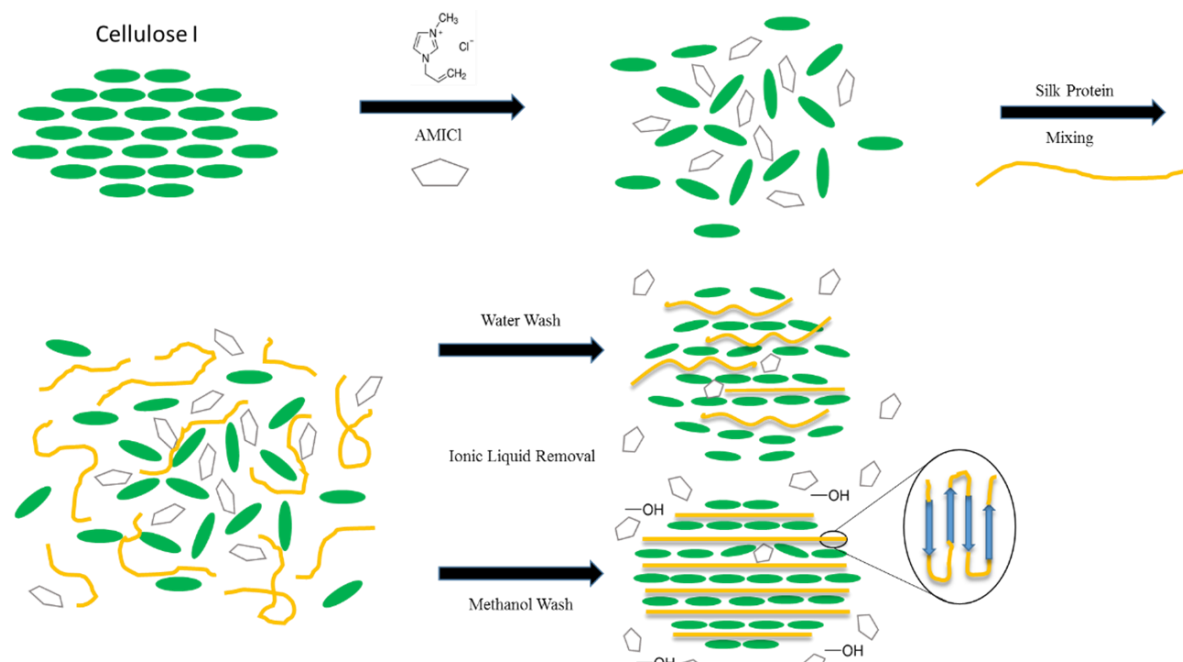
587

588 **Figure 5.** SEM images of regenerated cellulose fibers using ionic liquids and a water-based
 589 coagulation bath: (A) surface image; (B) cross-section image [100]. (Reproduced with permission from
 590 Ref. [100]; Copyright 2018 Wiley)

591 4.1.2. Methanol and other organic solvents

592 Methanol is a simple alcohol consisting of a methyl group linked to a hydroxyl group while
 593 ethanol, also known as ethyl alcohol, consists of an ethyl group linked to a hydroxyl group. Both
 594 alcohols are used to induce the formation of biopolymer fibers after ionic liquid dissolution. The
 595 highly polar agents act to remove the ionic liquid from the solution due to its hydroxyl (OH) group
 596 and high electronegativity of oxygen allowing hydrogen bonding to take place with other molecules.
 597 The attraction to non-polar molecules makes it an ideal solution to interact with the polar and non-
 598 polar regions of the biopolymers and ionic liquid, fusing the materials. In addition, the protein
 599 conformational transition change from random coil to β -sheet form are known to be induced by the
 600 methanol treatment.

601 The structural differences between using water or using methanol as a coagulation agent was
 602 observed in *Thai* silk-cellulose polymer (**Figure 6**) [102]. Thermal analysis showed that the thermal
 603 and physical properties could be finely tuned by manipulating hydrophobic-hydrophobic or
 604 electrostatic interactions between the silk and cellulose. Upon dissolution in ionic liquid, cellulose
 605 assumes a disordered structure with expanded fibrils that easily interact with silk molecules. After
 606 washing out ionic liquid with a coagulation agent, however, the unorganized cellulose reverts to a
 607 crystalline cellulose I structure with silk molecules inserted within, as confirmed by FTIR analysis.
 608 This process proceeds via immiscible phase separation. When methanol is used as a solvent, the silk
 609 components crystallize, resulting in a large number of β -sheets within the composite. Due to this,
 610 composites with any amount of silk will generally be mechanically superior to pure cellulose samples
 611 when treated with methanol instead of water. Further insight to these coagulation mechanisms open
 612 up the possibility of fine-tuning biopolymer composites through the use of different coagulation
 613 agents.



614

615 **Figure 6.** Water and methanol coagulation agents have different effects on the self-assembly of *Thai*
 616 silk-cellulose polymer composites. (Reproduced with permission from Ref. [102]; Copyright 2017
 617 Elsevier)

618 Most water-insoluble polysaccharide solutions can be coagulated in the both abovementioned
619 solvents (water or organic solvents). Protein solutions on the other hand are usually coagulated in
620 organic solvents such as alcohols since most proteins are soluble in water. In one study, ethanol was
621 used to regenerate cellulose/silk fibroin from N, N-dimethylacetamide/LiCl (DMAC/LiCl). Even
622 though there was no visible phase separation, micro-voids and a low degree of crystallinity in the
623 blend structures was reported [48]. Thus, it can be understood that these differences in blended
624 structures can be due to the different requirements of coagulation for silk fibroin and cellulose.

625 4.1.3. H₂O₂ Coagulation

626 Hydrogen peroxide (H₂O₂) is another chemical agent that induces the coagulation of
627 biopolymers. Hydrogen peroxide is the simplest peroxide consisting of an oxygen–oxygen single
628 bond. It is highly unstable and slowly decomposes in the presence of light. The mixture of hydrogen
629 peroxide and water is useful to wash out ionic liquids due to its interaction with the anions in the
630 solution and ability to form hydrogen bonds. Depending on its ratio of water to H₂O₂, its distinct use
631 on biopolymers such as cellulose induces a highly crystalline and brittle material.

632 In a study by Love et al [166], 1-ethyl-3-methylimidazolium acetate (EMIMAc) ionic liquid was
633 used to dissolve silk and cellulose into a composite biomaterial. The materials were then regenerated
634 with either water or varying percentages of hydrogen peroxide (1-25%). EMIMAc was able to
635 complete dissociate both silk and cellulose into solution and casted into thin films. Following casting,
636 the ionic liquid was easily washed out by the coagulation agent used, either water or hydrogen
637 peroxide. The impact of ionic liquid as a solvent on the material's morphological, thermal,
638 mechanical, and electrical properties was studied. Thermal and morphological analysis both showed
639 that a higher percentage of hydrogen peroxide promoted hydrogen bonding between hydroxide
640 groups on cellulose, resulting increased crystallinity and crystal size in the final biomaterial.

641 4.2. Effect of Ionic Liquid Ions on Fiber Structure and Ion Conductivity

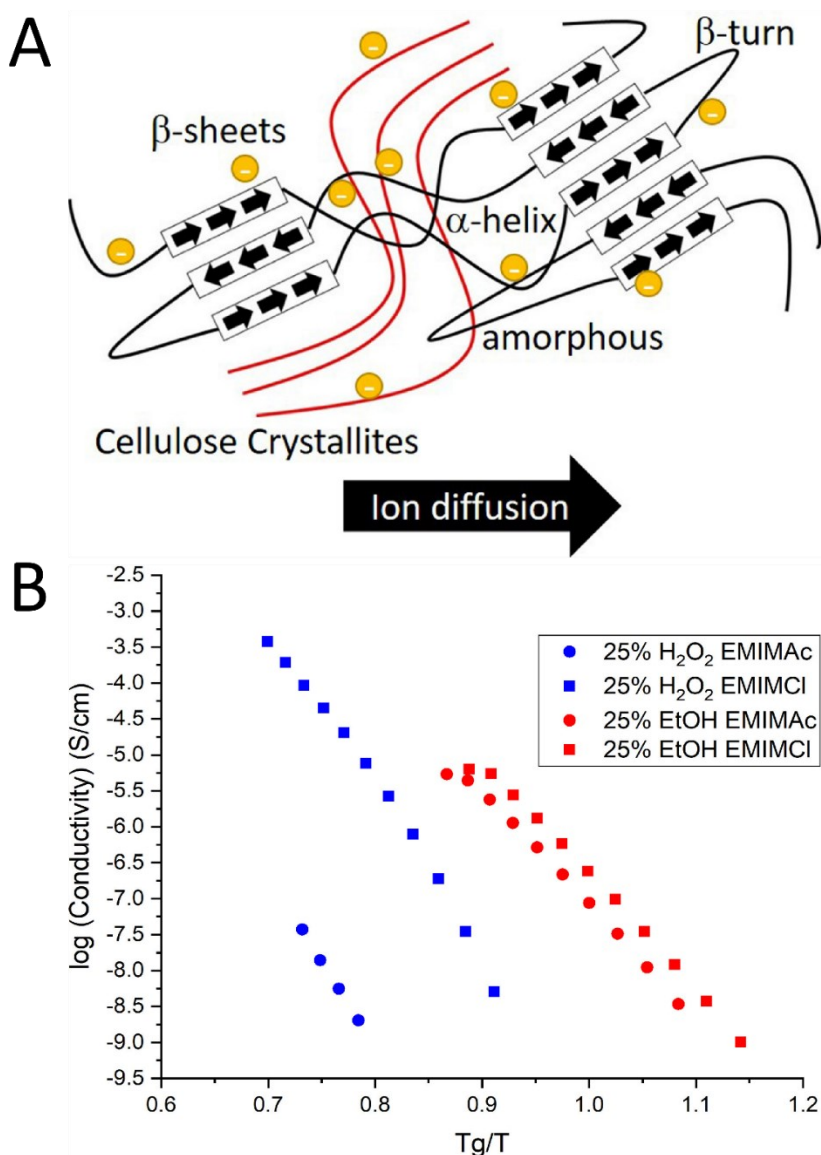
642 The inter- and intramolecular interactions between the anions of the ionic liquid and the
643 hydroxide groups in natural polymers can cause changes in the distribution of secondary structures
644 in the polymer. For example, using EMIMAc as a solvent will give a different protein sub-structure
645 than using EMIMCl due to different effects from the acetate anion or the chloride anion [25]. In this
646 study, using EMIMCl as a solvent resulted in more beta sheets in the final biomaterial compared to
647 using EMIMAc. Another study showed that bulkier anions, such as BMIMBr and BMIM-MeSO₃ can
648 increase molecular interactions because of their larger size. These molecular interactions include
649 electrostatic, hydrogen bonding, and hydrophobic-hydrophobic interactions between biopolymers in
650 solution [165]. Changing these structures leads to changes in the polymer's overall morphological,
651 thermal, and mechanical properties, indicating that ionic liquid choice can be used to tailor
652 biopolymers towards specific applications. Morphological changes also lead to ionic conductivity
653 modifications, which differed with the coagulation baths. These changes can influence the ionic
654 conductivity of the polymer in a way illustrated in **Figure 7**. Previous studies [167] have shown that
655 beta sheet content of proteins is correlated with ionic conductivity. Connecting these two ideas shows
656 how ionic liquid choices can be important in the production of batteries and bioelectronics.

657 In a similar study by Mahmood and colleagues [24] in a process termed “natural fiber welding”,
658 the ionic mobilizes fibrous polymers at their surface by disrupting hydrogen bonds. These mobile
659 materials are then intertwined with materials from neighboring fibers, and form a uniform layer after
660 removal of the ionic liquid solvent. Trulove et al utilized this process with *Bombyx mori* silk and hemp
661 thread. Their X-ray diffraction (XRD) and infrared (FTIR) results showed that significant amounts of
662 the native structure of the polymer was retained [168]. They go on to show that the most impactful
663 factor of this process was the amount and location of the modification to the polymer. Some
664 researchers have even used this technique to functionalize fibers at the surface using chemical
665 modifications to the molecule's sidechains [169, 170].

666 Mathematically, the morphology and structure of a polymer relate to its ability to dissociate ions
 667 through a combination of the Arrhenius equation and the Vogel-Fulcher-Tamman equation (1):

668
$$\sigma = qp_{\infty}\mu_{\infty} \exp\left(-\frac{E_a}{RT}\right) \exp\left[-\frac{B}{R(T-T_0)}\right] \quad (1)$$

669 In Equation 1, q is the charge of the ions, p_{∞} is the total ion density, μ_{∞} is ion mobility, E_a is the
 670 activation energy, T is the temperature, R is the universal gas constant, B is an energy barrier constant,
 671 and T_0 is the Vogel temperature [22, 171, 172]. The energy barrier constant B is a sum of the energy
 672 barrier for polymer segmental motion and the energy barrier of ion hopping [173]. The latter is worth
 673 discussing in the context of polymer morphology as it scales with the square of the hopping distance
 674 of the ion. This is true in both intramolecular and intermolecular motions, meaning the side-chain
 675 length of polymers, a function of protein substructure and polysaccharide side-chain groups, plays a
 676 significant role in the ionic conductivity of a biopolymer. In the context of IL, the energy barrier of
 677 ion hopping also scales with the size of the ion, which can be selected for when choosing an IL for a
 678 particular biomaterial. Another mechanism that affects ion diffusion and dissociation is the
 679 segmental movement of sidechains in the polymer [22, 174, 175]. All of these morphological processes
 680 can be attributed to the energy barrier constant in Equation 1, thus showing how the morphology of
 681 a polymer can have a massive effect on its ion conductivity. This concept is illustrated in Figure 7
 682 through different ILs ratios and different coagulation agents.



684 **Figure 7.** (A) Schematic representation of how ion diffusion through a solid electrolyte is dependent
685 on the molecular structure, including the content of various protein structures. (B) choice of
686 coagulation agent affects the morphology of a polymer, which in turn affects its ability to conduct
687 ions. Results are normalized to the glass transition temperature of each polymer. (Reproduced with
688 permission from Ref. [25]; Copyright 2019 Society of Chemical Industry)

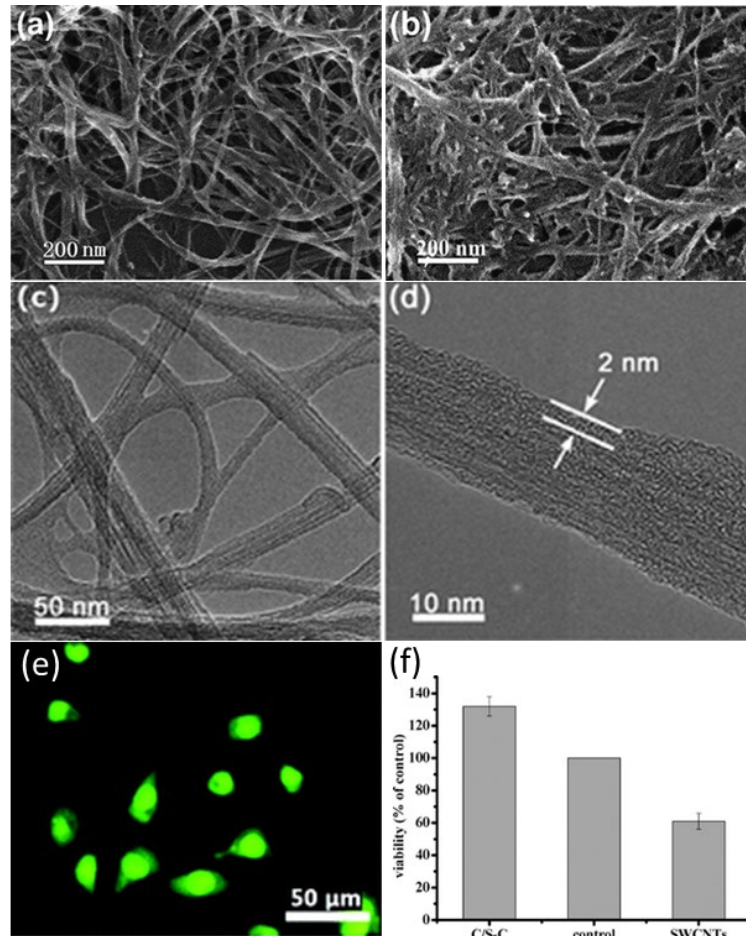
689 **5. Novel Applications of Biopolymer-Based Fibers from Ionic Liquids**

690 **5.1. Tissue Regeneration**

691 Ionic liquids have recently found their way into nanofibers intended for biomedical applications.
692 In 2014, AMIMCl was used as a solvent in the fabrication of a cellulose-based tissue engineering
693 scaffold with tunable microarchitecture [176]. These scaffolds were tested by culturing fibroblast cells
694 on them for 15 days to compare the biocompatibility of the samples to a control 2D cell culture dish.
695 A live/dead assay and DAPI staining were also performed to evaluate the biocompatibility *in vitro*.
696 Over 9 days, there was continuously a higher number of cells attached to the scaffold and MTT assay
697 confirmed that the cells were metabolically active. DAPI staining was also used to show cell
698 adherence to the scaffold.

699 In a similar vein of work, cellulose was able to be combined with single walled carbon nanotubes
700 (SWCNTs) in order to form a biomaterial with high biocompatibility [177]. This was accomplished in
701 part from cellulose's ability to easily dissolve in 1-butyl-3-methylimidazolium bromide (BMIMBr).
702 The cellulose/SWCNT complexes (C/S-Cs) were characterized through field emission SEM (Figure 8a
703 and 8b), high resolution TEM (Figure 8c and 8d), and FTIR. Their superior biocompatibility was
704 confirmed by WST-1 assay using HeLa cells as well as acridine orange (AO) and ethidium bromide
705 (EB) double staining. Figure 8e shows fluorescent microscopy of healthy HeLa cells growing on C/S-
706 Cs complexes. The lack of red EB dye indicates that no cells are in a necrotic state. Figure 8f shows
707 the results of the WST-1 assay, which shows a clear increase in cell viability in C/S-Cs complexes
708 compared to both glass microscope slides and purified SWCNTs without cellulose wrapping.

709



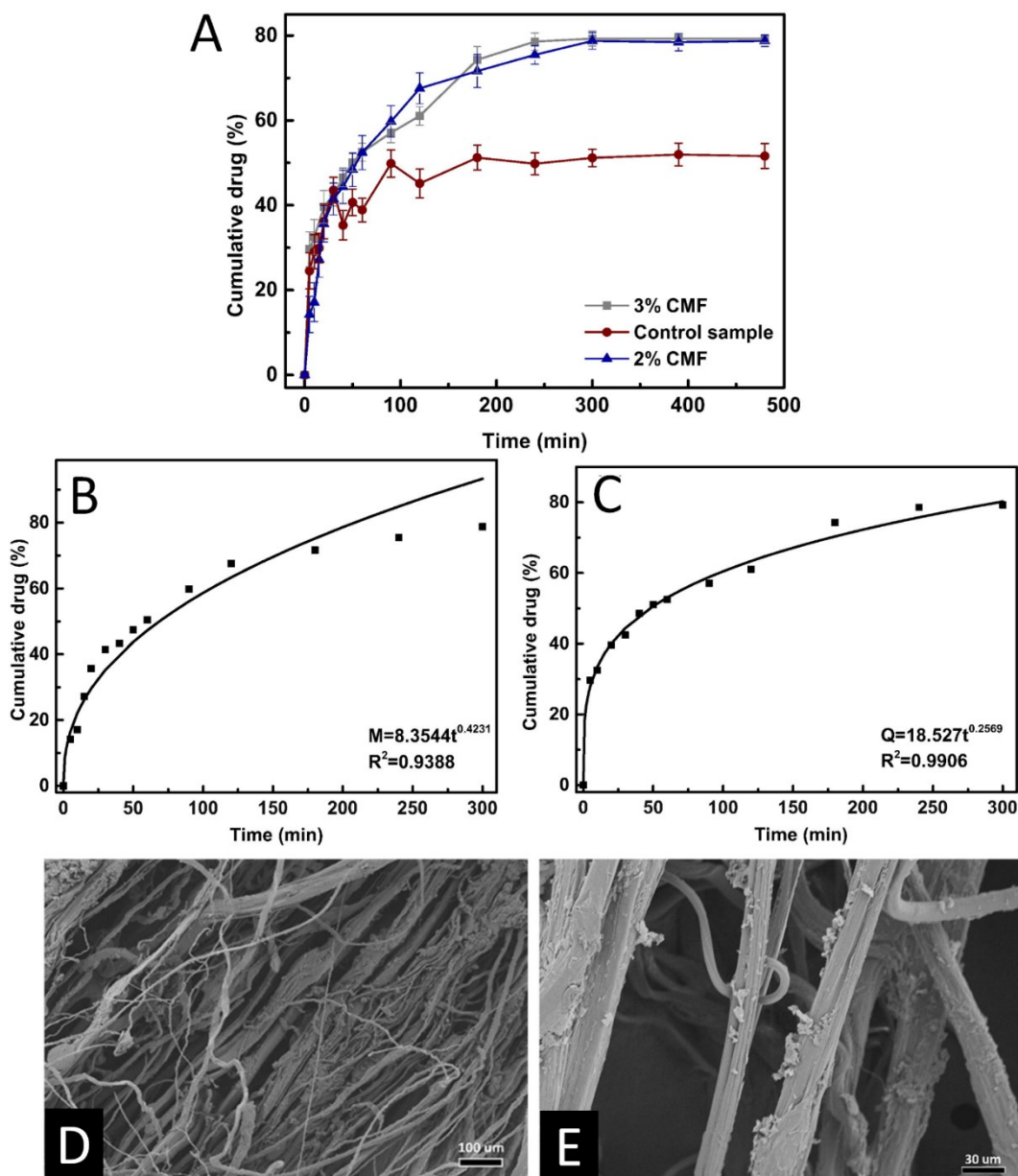
710

711 **Figure 8.** (A,B) Field emission SEM and (C,D) high resolution TEM micrographs of cellulose/SWCNT
 712 complexes (C/S-Cs) generated through a ionic liquid (BMIMBr); (E) fluorescent microscopy of HeLa
 713 cells after 24 hours of growth and AO/EB staining; (F) WST-1 assay shows a significant increase in
 714 HeLa cell viability on C/S-C. (Reproduced with permission from Ref. [177]; Copyright 2009 The Royal
 715 Society of Chemistry)

716 *5.2. Drug Delivery*

717 An area of expertise for nanofibers formed from ionic liquids is topical drug delivery. To cite a
 718 specific example, Liu and colleagues electrospun fibrous membranes from regenerated cellulose
 719 dissolved in 1-butyl-3-methylimidazolium chloride (BMIMCl) (Figure 9) [178]. The resulting
 720 cellulose micro-nano fiber (CMF) matrix was soaked in a solution of ibuprofen in ethanol in order to
 721 load them with the drug to test its capabilities as a drug carrier. Material characterization was
 722 performed through SEM, FTIR, TGA, tribological testing wettability and contact angle testing, 24-
 723 hour cell viability assay, and a drug release assay. Nanofiber diameters ranged from the under 1 μ m
 724 to around 20 μ m with limited morphological differences between 2 and 3% wt/vol of ibuprofen. At
 725 2%, however, there was notable fusion occurred between ionic liquid surfaces and water surfaces due
 726 to the ionic liquid not washing off fast enough during the electrospinning process. This fusion was
 727 mostly absent in the 3% samples. At 3%, the integration of ibuprofen shifted the thermal degradation
 728 of the fiber matrixes slightly higher due to hydrogen bonding. Tribological testing was performed
 729 with the intent to minimize roughness which would irritate the skin if the fibers were used as a
 730 bandage. Overall, the research determined through coefficients of friction that the surface roughness
 731 was lower than that of other electrospun fibers and drug loading did not significantly increase the
 732 coefficient. SEM images of these fibers are shown in Figure 9D and Figure 9E with different scale
 733 bars. A 24-hour cell-viability test classified the materials as qualified biomaterials under the *United*
 734 *States Pharmacopeia* with a higher viability than a control cellulose material. After this qualification, a

735 drug release study was done under physiological conditions of 37 °C and 5.5 pH to mimic the
 736 conditions on human skin. In order to model the release of ibuprofen, the drug release was plotted
 737 and fitted to a curve based on Peppas equation. The results for both of these studies are plotted in
 738 Figure 9A-C. Release exponents of 0.42 and 0.25 for the 2% and 3% IBU samples, respectively, indicate
 739 that both drug releases were controlled by Fickian diffusion through the CMF matrices. The fiber
 740 samples exhibited a biphasic release, with a quick initial release for 100 minutes followed by a slower
 741 release to a cumulative 80% drug release for the last 200 minutes. The researchers note that this time
 742 is ideal for other drug carriers loaded by simple immersing, and that they have the potential to be
 743 reloaded and reused.



744

745 **Figure 9.** Drug release profiles for (A) IBU@2% CMF and IBU@3% CMF matrices compared to a
 746 control tea bag and the curve fits based on Peppas equation for the (B) 2% and (C) 3% samples;
 747 (D,E) SEM images cellulose micro-nano (CMF) fibers IBU@3% matrices. (Reproduced with permission
 748 from Ref. [178]; Copyright 2017 Elsevier)

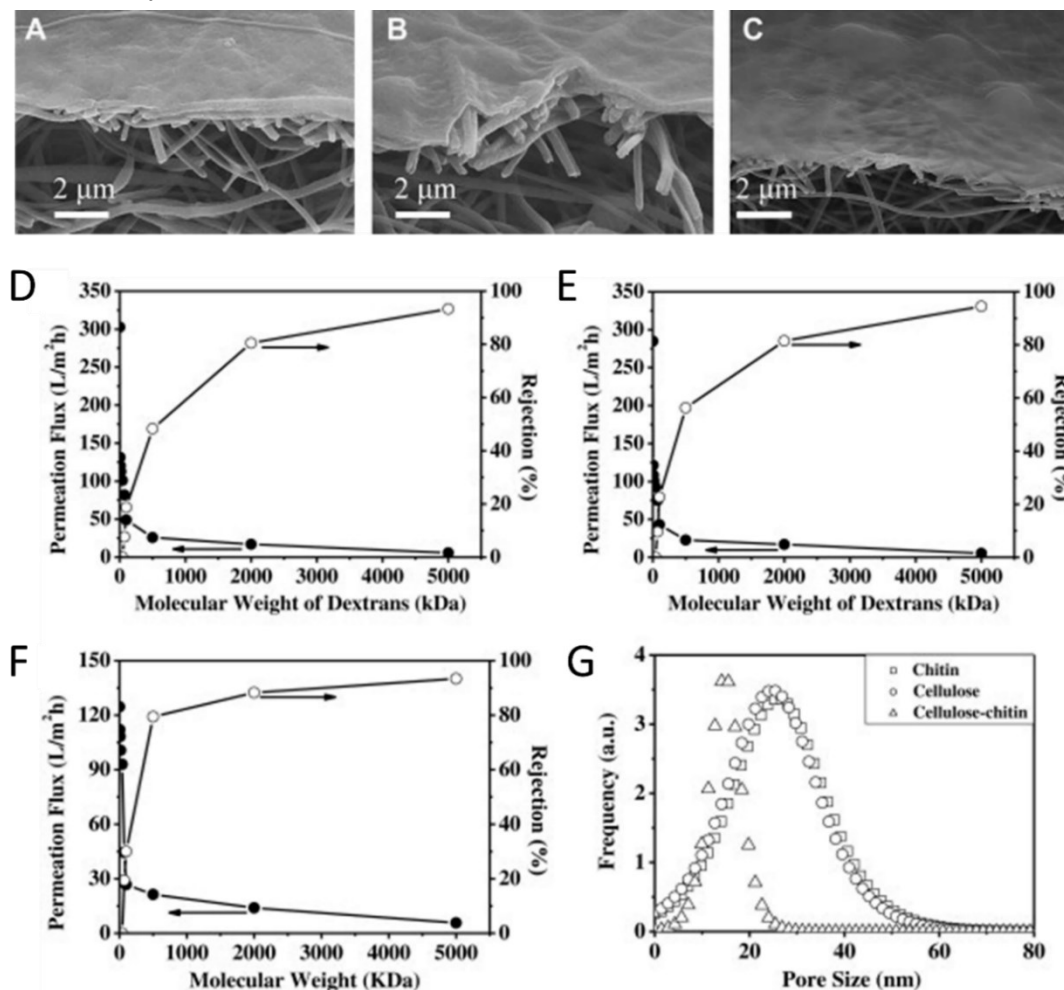
749 5.5. Water Purification

750 Polysaccharides, including cellulose, have seen increasing use as a material in wastewater filters
 751 recently. However, since cellulose can be digested by microorganisms, it can be combined with chitin,
 752 which is more bioinert, to form the barrier layer of a nanofibrous scaffold for filtration. SEM images
 753 of this barrier layer are shown in **Figure 10** for cellulose, chitin, and chitin-cellulose composite barrier
 754 layers. High-flux thin-film nanofibrous composite (TFNC) membranes were created using chitin,
 755 cellulose, and chitin-cellulose composites regenerated from 1-ethyl-3-methylimidazolium acetate
 756 (EAc) [179]. The dissolution was then added to ethanol to regenerate the polysaccharide structure.
 757 Normally, microcrystalline cellulose is too crystalline to be processed into membranes [180], but the
 758 analysis done in this study shows that cellulose and chitin can be used as a barrier layer for
 759 membranes since the layer was less than 500 nm thick. The membranes fabricated were able to take
 760 advantage of the properties of cellulose and chitin to produce membranes with high permeation flux
 761 and high rejection ratio compared to commercially available membranes. Figure 10D-F also compares
 762 cellulose, chitin, and chitin-cellulose composite TFNC membranes membrane to show a high
 763 permeation flux and a comparable rejection ratio. Figure 10G compares the distribution of pore sizes
 764 in the three membranes. The rejection ratio $R\%$ was calculated by equation (2):

$$765 R\% = \frac{C_f - C_p}{C_f} * 100\% \quad (2)$$

766 where C_f is the concentration of the feed solution and C_p is the concentration of the permeation
 767 solution.

768 In addition to the successful membrane product, the ionic liquid used in this study was able to
 769 be recovered a re-used via distillation at atmospheric pressure. ^1H nuclear magnetic resonance (NMR)
 770 spectroscopy confirmed the purity of the recycled ionic liquid within 2% impurity, which had no
 771 effect on its ability to re-dissolve chitin.

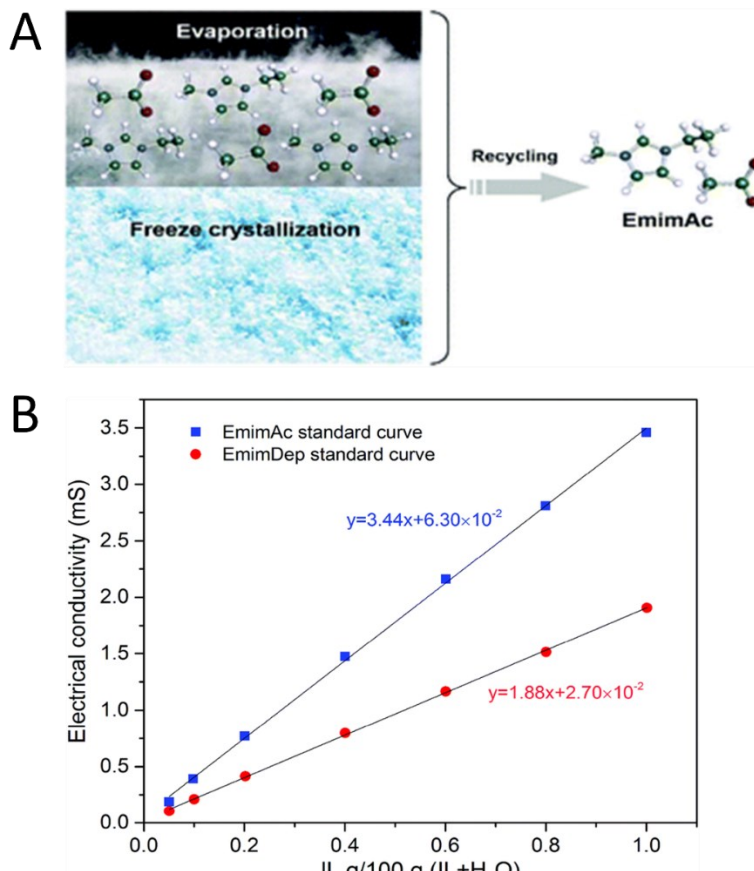


773 **Figure 10.** Cross-section SEM images of (A) cellulose, (B) chitin, and (C) cellulose–chitin blend barrier
 774 layers prepared by ionic liquid regeneration in 1-ethyl-3-methylimidazolium acetate. Graphs (D–
 775 F) show the permeation flux and rejection ratios of (D) cellulose, (E) chitin, and (F) chitin-cellulose
 776 composite membranes, while (G) compares the distribution of pore sizes in the membranes.
 777 (Reproduced with permission from Ref. [179]; Copyright 2011 Elsevier).

778 **5.6 Recycling of Ionic Liquid**

779 One of the most valuable aspects of using ionic liquids as a solvent appeals to its inherent green
 780 chemistry. After use, ionic liquids can easily be recovered and reused by adding non-solvents such
 781 as water or acetone and then evaporating the non-solvent to recover the ionic liquid that was used
 782 such as in **Figure 11** [181, 182]. Ongoing studies are being done to select suitable non-solvents that
 783 maximize the yield of recovered ionic liquid and reduce the overall cost of processing biomass into
 784 useful forms. Some methods of recovering ionic liquid currently being studied include column
 785 chromatography based on solid adsorption properties [183] with organic solvents and a combination
 786 of freeze crystallization and evaporation [101] of water in a mixture of ionic liquid and water.

787 In one particular example, evaporation and freeze drying were utilized to recover EMIMAc and
 788 EMIMDep during the process of cellulose nanofiber formation. A graphical abstract is shown in
 789 Figure 11A. Enthalpies involved in each step of the recovery process were used to calculate the energy
 790 consumption required to recover the ionic liquid used per kilogram of cellulose dissolved. These
 791 calculations also relied on the assumptions that freeze drying had an efficiency of 60% while vacuum
 792 drying and the evaporation process were 100% efficient. Their calculations show that using freeze
 793 drying prior to evaporation of ionic liquid, compared to simply evaporating ionic liquid, is a more
 794 energy efficient process for the recycling of ionic liquid. The recycling process was highly effective,
 795 where EMIMAc and EMIMDep regenerated solvents contained 94.2% and 94.8%, of the original
 796 amount of solvent, respectively. These values were determined by the electrical conductivity of the
 797 regenerated solvents using a standard calibration curve for each ionic liquid, shown in Figure 11B.



799 **Figure 11.** (A) A combination of evaporation and freeze crystallization is used to separate and recover
800 ionic liquid mixed with water in this cellulose nanofiber fabrication method. (B) Standard conductivity
801 curves for EMIMAc and EMIMDep used to determine the concentration of ionic liquid in the
802 regenerated solvents. (Reproduced with permission from Ref. [101]; Copyright The Royal Society of
803 Chemistry)

804 **5.7 Electromechanical Actuators**

805 An important component of electroactive polymers (EAP) are electromechanical actuators.
806 Many novel EAPs are fabricated using ionic liquids as a dopant within EAP materials. Ionic liquids
807 with cations of large Van der Walls volumes (e.g. $[C_2mim][Tf]$, $[TES][NTf_2]$, $[BMP][NTf_2]$, and
808 $[C_2mim][Cl]$) have been used as dopants to enhance cationic strain [184], while others like
809 $[C_2mim][PF_6]$ and $[C_6mim][PF_6]$ are used in actuators to generate large strains of up to 4% [185]. By
810 combining EAPs with ionic liquids, biocompatible electromechanical actuators have been fabricated
811 with effective bending actuation and tunable mechanical properties [184]. Previous to the use of ionic
812 liquids, EAP would require the use of an electrolyte solution to function properly. The recent use of
813 ionic liquids in this field, combined with ionic liquid's potential as a solvent in fiber formation, shows
814 large potential for bioactive polymers as implants or in medical devices.

815 **6. Conclusion**

816 Fiber materials created from natural macromolecules hold great promise in several fields
817 including medicine, green chemistry, and bioelectronics. The molecular structure of these fibrous
818 materials can be fine-tuned for specific applications using specific solvents and preparation methods.
819 Recently, the use of ionic liquid as a solvent or in the processing of materials has shown great promise
820 in optimizing and functionalizing biomaterials. Understanding the mechanisms behind fiber
821 formation and biopolymer interactions in ionic liquid will help guide fiber materials into more
822 organized, multi-level 1D fiber materials or fiber matrices for many uses. Using the wide range of
823 ionic liquids and fiber preparation and processing techniques, fiber materials from natural sources
824 have become more robust than ever while maintaining or improving their green footprints.

825 **Author Contributions:** All authors contributed to the writing of this review paper; Review & Editing, C.R.G. and
826 X.H. All authors have read and agreed to the published version of the manuscript.

827 **Funding:** This study was supported by NSF Biomaterials Program (DMR-1809354 and DMR-1809541).

828 **Conflicts of Interest:** The authors declare no conflict of interest.

829 **References**

1. Mohan, T.; Čas, A.; Bračić, M.; Plohl, O.; Vesel, A.; Rupnik, M.; Zemljič, L. F.; Rebol, J., Highly Protein Repellent and Antiadhesive Polysaccharide Biomaterial Coating for Urinary Catheter Applications. *ACS Biomaterials Science and Engineering* **2019**, 5, (11), 5825-5832.
2. David, K., Advances and challenges with fibrous protein biomaterial designs. *Frontiers in Bioengineering and Biotechnology* **2016**, 4.
3. *Polysaccharide Based Graft Copolymers*. 1st ed. 2013. ed.; Springer Berlin Heidelberg: Berlin, Heidelberg, 2013.
4. *Protein-based Engineered Nanostructures*. 1st ed. 2016. ed.; Springer International Publishing: Cham, 2016.
5. Toita, S.; Morimoto, N.; Akiyoshi, K., Functional cycloamylose as a polysaccharide-based biomaterial: application in a gene delivery system. *Biomacromolecules* **2010**, 11, (2), 397-401.
6. Wang, Y.; Kotsuchibashi, Y.; Liu, Y.; Narain, R., Temperature-responsive hyperbranched amine-based polymers for solid-liquid separation. *Langmuir : the ACS journal of surfaces and colloids* **2014**, 30, (9), 2360-2368.

842 7. Villmow, T.; Pegel, S.; Pötschke, P.; Heinrich, G., Polymer/carbon nanotube composites for liquid sensing:
843 Model for electrical response characteristics. *Polymer* **2011**, *52*, (10), 2276-2285.

844 8. Villmow, T.; John, A.; Pötschke, P.; Heinrich, G., Polymer/carbon nanotube composites for liquid sensing:
845 Selectivity against different solvents. *Polymer* **2012**, *53*, (14), 2908-2918.

846 9. Leipzig, N. D.; Wylie, R. G.; Kim, H.; Shoichet, M. S., Differentiation of neural stem cells in three-
847 dimensional growth factor-immobilized chitosan hydrogel scaffolds. *Biomaterials* **2011**, *32*, (1), 57-64.

848 10. Hayden, R. S.; Quinn, K. P.; Alonzo, C. A.; Georgakoudi, I.; Kaplan, D. L., Quantitative characterization of
849 mineralized silk film remodeling during long-term osteoblast–osteoclast co-culture. *Biomaterials* **2014**, *35*,
850 (12), 3794-3802.

851 11. Hubbell, J. A.; Chilkoti, A., Chemistry. Nanomaterials for drug delivery. *Science (New York, N.Y.)* **2012**, *337*,
852 (6092), 303-305.

853 12. Mottaghitalab, F.; Farokhi, M.; Shokrgozar, M. A.; Atyabi, F.; Hosseinkhani, H., Silk fibroin nanoparticle
854 as a novel drug delivery system. *Journal of Controlled Release* **2015**, *206*, 161-176.

855 13. Yewale, C.; Baradia, D.; Vhora, I.; Misra, A., Proteins: emerging carrier for delivery of cancer therapeutics.
856 *Expert Opinion on Drug Delivery* **2013**, *10*, (10), 1429-1448.

857 14. Pattamaprom, C.; Hongrojanawiwat, W.; Koombhongse, P.; Supaphol, P.; Jarusuwannapoo, T.;
858 Rangkupan, R., The Influence of Solvent Properties and Functionality on the Electrospinnability of
859 Polystyrene Nanofibers. *Macromolecular Materials and Engineering* **2006**, *291*, (7), 840-847.

860 15. Wu, X.; Wang, L.; Yu, H.; Huang, Y., Effect of solvent on morphology of electrospinning ethyl cellulose
861 fibers. *Journal of Applied Polymer Science* **2005**, *97*, (3), 1292-1297.

862 16. Lu, C.; Chen, P.; Li, J.; Zhang, Y., Computer simulation of electrospinning. Part I. Effect of solvent in
863 electrospinning. *Polymer* **2006**, *47*, (3), 915-921.

864 17. Liu, Q.; Wang, F.; Gu, Z.; Ma, Q.; Hu, X., Exploring the Structural Transformation Mechanism of Chinese
865 and Thailand Silk Fibroin Fibers and Formic-Acid Fabricated Silk Films. *International journal of molecular
866 sciences* **2018**, *19*, (11).

867 18. Fox, D.; Fylstra, P.; Hanley, M.; Henderson, W. A.; Trulove, P. C.; Bellayer, S.; Gilman, J.; De Long, H. C. In
868 *The Preparation and Characterization of Bombyx Mori Silk Nanocomposites Using Ionic Liquids*, ECS
869 Transactions, 2007; ECS: 2007.

870 19. Park, T.-J.; Jung, Y. J.; Choi, S.-W.; Park, H.; Kim, H.; Kim, E.; Lee, S. H.; Kim, J. H., Native chitosan/cellulose
871 composite fibers from an ionic liquid via electrospinning. *Macromolecular Research* **2011**, *19*, (3), 213-215.

872 20. Viswanathan, G.; Murugesan, S.; Pushparaj, V.; Nalamasu, O.; Ajayan, P. M.; Linhardt, R. J., Preparation
873 of Biopolymer Fibers by Electrospinning from Room Temperature Ionic Liquids. *Biomacromolecules* **2006**, *7*,
874 (2), 415-418.

875 21. Meli, L.; Miao, J.; Dordick, J. S.; Linhardt, R. J., Electrospinning from room temperature ionic liquids for
876 biopolymer fiber formation. *Green Chemistry* **2010**, *12*, (11), 1883-1892.

877 22. Lee, M.; Choi, U. H.; Colby, R. H.; Gibson, H. W., Ion Conduction in Imidazolium Acrylate Ionic Liquids
878 and their Polymers. *Chemistry of Materials* **2010**, *22*, (21), 5814-5822.

879 23. Stanton, J.; Xue, Y.; Pandher, P.; Malek, L.; Brown, T.; Hu, X.; Salas-de la Cruz, D., Impact of ionic liquid
880 type on the structure, morphology and properties of silk-cellulose biocomposite materials. *International
881 Journal of Biological Macromolecules* **2018**, *108*, 333-341.

882 24. Mahmood, H.; Moniruzzaman, M.; Yusup, S.; Welton, T., Ionic liquids assisted processing of renewable
883 resources for the fabrication of biodegradable composite materials. *Green Chemistry* **2017**, *19*, (9), 2051-2075.

884 25. Blessing, B.; Trout, C.; Morales, A.; Rybacki, K.; Love, S. A.; Lamoureux, G.; O'Malley, S. M.; Hu, X.; Salas-
885 de la Cruz, D., Morphology and ionic conductivity relationship in silk/cellulose biocomposites. *Polymer*
886 *International* **2019**, *68*, (9), 1580-1590.

887 26. Blessing, B.; Trout, C.; Morales, A.; Rybacki, K.; Love, S. A.; Lamoureux, G.; O'Malley, S. M.; Hu, X.; Salas -
888 de la Cruz, D., Morphology and ionic conductivity relationship in silk/cellulose biocomposites. *Polymer*
889 *International* **2019**, *68*, (9), 1580-1590.

890 27. Luzio, A.; Canesi, E.; Bertarelli, C.; Caironi, M., Electrospun Polymer Fibers for Electronic Applications.
891 *Materials* **2014**, *7*, (2), 906-947.

892 28. Han, Y.-L.; Xu, Q.; Lu, Z.; Wang, J.-Y., Cell adhesion on zein films under shear stress field. *Colloids and*
893 *Surfaces B: Biointerfaces* **2013**, *111*, 479-485.

894 29. Dhyani, V.; Singh, N., Controlling the cell adhesion property of silk films by graft polymerization. *ACS*
895 *applied materials & interfaces* **2014**, *6*, (7), 5005-5011.

896 30. Sutherland, T. D.; Young, J. H.; Weisman, S.; Hayashi, C. Y.; Merritt, D. J., Insect silk: one name, many
897 materials. *Annu Rev Entomol* **2010**, *55*, 171-88.

898 31. Extracellular fibrous proteins: the silks. *Comprehensive Biochem* **1968**, *26*, (B), 475-558.

899 32. Florkin, M., *Comparative Biochemistry V4: A Comprehensive Treatise*. Elsevier Science: 2012.

900 33. Rudall, K. M.; Kenchington, W., Arthropod Silks: The Problem of Fibrous Proteins in Animal Tissues.
901 *Annual Review of Entomology* **1971**, *16*, (1), 73-96.

902 34. Slotta, U.; Tammer, M.; Kremer, F.; Koelsch, P.; Scheibel, T., Structural Analysis of Spider Silk Films.
903 *Supramolecular Chemistry: Special Issue on Supramolecular Biochemical Assemblies* **2006**, *18*, (5), 465-471.

904 35. Hu, X.; Raja, W. K.; An, B.; Tokareva, O.; Cebe, P.; Kaplan, D. L., Stability of Silk and Collagen Protein
905 Materials in Space. In.

906 36. Wang, C.; Wu, S.; Jian, M.; Xie, J.; Xu, L.; Yang, X.; Zheng, Q.; Zhang, Y., Silk nanofibers as high efficient
907 and lightweight air filter. *Nano Research* **2016**, *9*, (9), 2590-2597.

908 37. Cohen-Karni, T.; Jeong, K. J.; Tsui, J. H.; Reznor, G.; Mustata, M.; Wanunu, M.; Graham, A.; Marks, C.; Bell,
909 D. C.; Langer, R.; Kohane, D. S., Nanocomposite gold-silk nanofibers. *Nano letters* **2012**, *12*, (10), 5403-5406.

910 38. Dinis, T. M.; Vidal, G.; Jose, R. R.; Vigneron, P.; Bresson, D.; Fitzpatrick, V.; Marin, F.; Kaplan, D. L.; Egles,
911 C., Complementary effects of two growth factors in multifunctionalized silk nanofibers for nerve
912 reconstruction. *PloS one* **2014**, *9*, (10), e109770-e109770.

913 39. Wenk, E.; Merkle, H. P.; Meinel, L., Silk fibroin as a vehicle for drug delivery applications. *Journal of*
914 *Controlled Release* **2011**, *150*, (2), 128-141.

915 40. Reeves, A. R. D.; Spiller, K. L.; Freytes, D. O.; Vunjak-Novakovic, G.; Kaplan, D. L., Controlled release of
916 cytokines using silk-biomaterials for macrophage polarization. *Biomaterials* **2015**, *73*, 272-283.

917 41. Asakura, T.; Miller, T., *Biotechnology of Silk*. Springer Netherlands: 2013.

918 42. Chun, H. J.; Park, K.; Kim, C. H.; Khang, G., *Novel Biomaterials for Regenerative Medicine*. Springer Singapore:
919 2018.

920 43. Yin, Z.; Jian, M.; Wang, C.; Xia, K.; Liu, Z.; Wang, Q.; Zhang, M.; Wang, H.; Liang, X.; Liang, X.; Long, Y.;
921 Yu, X.; Zhang, Y., Splash-Resistant and Light-Weight Silk-Sheathed Wires for Textile Electronics. *Nano*
922 *letters* **2018**, *18*, (11), 7085.

923 44. Kim, D.-H.; Kim, Y.-S.; Amsden, J.; Panilaitis, B.; Kaplan, D. L.; Omenetto, F. G.; Zakin, M. R.; Rogers, J. A.,
924 Erratum: "Silicon electronics on silk as a path to bioresorbable, implantable devices" [*Appl. Phys. Lett.* **95**
925 , 133701 (2009)]. *Applied Physics Letters* **2009**, *95*, (26).

926 45. Dae-Hyeong, K.; Jonathan, V.; Jason, J. A.; Jianliang, X.; Leif, V.; Yun-Soung, K.; Justin, A. B.; Bruce, P.; Eric, S. F.; Diego, C.; David, L. K.; Fiorenzo, G. O.; Yonggang, H.; Keh-Chih, H.; Mitchell, R. Z.; Brian, L.; John, A. R., Dissolvable films of silk fibroin for ultrathin conformal bio-integrated electronics. *Nature Materials* 2010, 9, (6), 511.

927 46. Phillips, D. M.; Drummy, L. F.; Naik, R. R.; Long, H. C. D.; Fox, D. M.; Trulove, P. C.; Mantz, R. A., Regenerated silk fiber wet spinning from an ionic liquid solution. *Journal of Materials Chemistry* 2005, 15, (39), 4206-4208.

928 47. Shen, X., Regeneration spider silk fiber based on ionic liquid and preparation method of regeneration spider silk fiber. In 2015.

929 48. Yao, Y.; Mukuze, K. S.; Zhang, Y.; Wang, H., Rheological behavior of cellulose/silk fibroin blend solutions with ionic liquid as solvent. *Cellulose* 2014, 21, (1), 675-684.

930 49. Zhou, L.; Wang, Q.; Wen, J.; Chen, X.; Shao, Z., Preparation and characterization of transparent silk fibroin/cellulose blend films. *Polymer* 2013, 54, (18), 5035-5042.

931 50. Aluigi, A.; Corbellini, A.; Rombaldoni, F.; Mazzuchetti, G., Wool-derived keratin nanofiber membranes for dynamic adsorption of heavy-metal ions from aqueous solutions. *Textile Research Journal* 2013, 83, (15), 1574-1586.

932 51. Lee, C.-H.; Yun, Y. J.; Cho, H.; Lee, K. S.; Park, M.; Kim, H. Y.; Son, D. I., Environment-friendly, durable, electro-conductive, and highly transparent heaters based on silver nanowire functionalized keratin nanofiber textiles. *Journal of Materials Chemistry C* 2018, 6, (29), 7847-7854.

933 52. Atri, H.; Bidram, E.; Dunstan, D. E., Reconstituted Keratin Biomaterial with Enhanced Ductility. *Materials (Basel)* 2015, 8, (11), 7472-7485.

934 53. Cui, L.; Gong, J.; Fan, X.; Wang, P.; Wang, Q.; Qiu, Y., Transglutaminase - modified wool keratin film and its potential application in tissue engineering. *Engineering in Life Sciences* 2013, 13, (2), 149-155.

935 54. Feng, Y.; Borrelli, M.; Meyer-Ter-Vehn, T.; Reichl, S.; Schrader, S.; Geerling, G., Epithelial Wound Healing on Keratin Film, Amniotic Membrane and Polystyrene In Vitro. *Current Eye Research* 2014, 39, (6), 561-570.

936 55. Lusiana; Reichl, S.; Müller-Goymann, C. C., Keratin film made of human hair as a nail plate model for studying drug permeation. *European Journal of Pharmaceutics and Biopharmaceutics* 2011, 78, (3), 432-440.

937 56. Ramirez, D. O. S.; Carletto, R. A.; Tonetti, C.; Giachet, F. T.; Varesano, A.; Vineis, C., Wool keratin film plasticized by citric acid for food packaging. *Food Packaging and Shelf Life* 2017, 12, 100-106.

938 57. Murrell, D. F.; Trisnowati, N.; Miyakis, S.; Paller, A. S., The Yin and the Yang of Keratin Amino Acid Substitutions and Epidermolysis Bullosa Simplex. *Journal of Investigative Dermatology* 2011, 131, (9), 1787-1790.

939 58. Chen, J.; Vongsanga, K.; Wang, X.; Byrne, N., What Happens during Natural Protein Fibre Dissolution in Ionic Liquids. *Materials* 2014, 7, (9), 6158-6168.

940 59. Li, R.; Wang, D., Preparation of regenerated wool keratin films from wool keratin-ionic liquid solutions. *Journal of Applied Polymer Science* 2013, 127, (4), 2648-2653.

941 60. Wool, R.; Sun, X. S., *Bio-Based Polymers and Composites*. Elsevier Science: 2011.

942 61. Liu, X.; Souzandeh, H.; Zheng, Y.; Xie, Y.; Zhong, W.-H.; Wang, C., Soy protein isolate/bacterial cellulose composite membranes for high efficiency particulate air filtration. *Composites Science and Technology* 2017, 138, 124-133.

943 62. Kang, H.-J.; Kim, S.-J.; You, Y.-S.; Lacroix, M.; Han, J., Inhibitory effect of soy protein coating formulations on walnut (*Juglans regia* L.) kernels against lipid oxidation. *LWT - Food Science and Technology* 2013, 51, (1), 393-396.

969 63. Peles, Z.; Binderman, I.; Berdichevsky, I.; Zilberman, M., Soy protein films for wound - healing applications:
970 antibiotic release, bacterial inhibition and cellular response. *Journal of Tissue Engineering and Regenerative
971 Medicine* **2013**, *7*, (5), 401-412.

972 64. Chuysinuan, P.; Pengsuk, C.; Lirdprapamongkol, K.; Techasakul, S.; Svasti, J.; Nooeaid, P., Enhanced
973 Structural Stability and Controlled Drug Release of Hydrophilic Antibiotic-Loaded Alginate/Soy Protein
974 Isolate Core-Sheath Fibers for Tissue Engineering Applications. *Fibers and Polymers* **2019**, *20*, (1), 1-10.

975 65. Noshad, M.; Mohebbi, M.; Koocheki, A.; Shahidi, F., Microencapsulation of vanillin by spray drying using
976 soy protein isolate–maltodextrin as wall material. *Flavour and Fragrance Journal* **2015**, *30*, (5), 387-391.

977 66. Wu, R. L.; Wang, X. L.; Wang, Y. Z.; Bian, X. C.; Li, F., Cellulose/soy protein isolate blend films prepared
978 via room-temperature ionic liquid. *Industrial and Engineering Chemistry Research* **2009**, *48*, (15), 7132-7136.

979 67. Li, C.; He, M.; Tong, Z.; Li, Y.; Sheng, W.; Luo, L.; Tong, Y.; Yu, H.; Huselstein, C.; Chen, Y., Construction
980 of biocompatible regenerated cellulose/SPI composite beads using high-voltage electrostatic technique.
981 *RSC Advances* **2016**, *6*, (58), 52528-52538.

982 68. Brennan, A. B.; Kirschner, C. M.; Kirschner, C. M., *Bio-Inspired Materials for Biomedical Engineering*. John
983 Wiley & Sons, Incorporated: Somerset, UNITED STATES, 2014.

984 69. Meng, Z.; Zheng, X.; Tang, K.; Liu, J.; Ma, Z.; Zhao, Q., Dissolution and regeneration of collagen fibers
985 using ionic liquid. *International Journal of Biological Macromolecules* **2012**, *51*, (4), 440-448.

986 70. Pei, Y.; Chu, S.; Zheng, Y.; Zhang, J.; Liu, H.; Zheng, X.; Tang, K., Dissolution of Collagen Fibers from
987 Tannery Solid Wastes in 1-Allyl-3-methylimidazolium Chloride and Modulation of Regenerative
988 Morphology. *ACS Sustainable Chemistry and Engineering* **2019**, *7*, (2), 2530-2537.

989 71. Tarannum, A.; Muvva, C.; Mehta, A.; Rao, J. R.; Fathima, N. N., Phosphonium based ionic liquids-
990 stabilizing or destabilizing agents for collagen? *RSC Advances* **2016**, *6*, (5), 4022-4033.

991 72. Wise, S. G.; Weiss, A. S., Tropoelastin. *The International Journal of Biochemistry & Cell Biology* **2009**, *41*, (3),
992 494-497.

993 73. Csiszar, K., Lysyl oxidases: A novel multifunctional amine oxidase family. In *Progress in Nucleic Acid
994 Research and Molecular Biology*, Academic Press: 2001; Vol. 70, pp 1-32.

995 74. Waterhouse, A.; Wise, S. G.; Ng, M. K. C.; Weiss, A. S., Elastin as a Nonthrombogenic Biomaterial. *Tissue
996 Engineering Part B: Reviews* **2011**, *17*, (2), 93-99.

997 75. Daamen, W. F.; Veerkamp, J. H.; van Hest, J. C. M.; van Kuppevelt, T. H., Elastin as a biomaterial for tissue
998 engineering. *Biomaterials* **2007**, *28*, (30), 4378-4398.

999 76. Wright, E. R.; McMillan, R. A.; Cooper, A.; Apkarian, R. P.; Conticello, V. P., Thermoplastic Elastomer
1000 Hydrogels via Self-Assembly of an Elastin-Mimetic Triblock Polypeptide. *Advanced Functional Materials*
1001 **2002**, *12*, (2), 149-154.

1002 77. Mithieux, S. M.; Rasko Je Fau - Weiss, A. S.; Weiss, A. S., Synthetic elastin hydrogels derived from massive
1003 elastic assemblies of self-organized human protein monomers. *Biomaterials* **2004**, *25*(20), (0142-9612 (Print)).

1004 78. Herrero-Vanrell, R.; Rincon Ac Fau - Alonso, M.; Alonso M Fau - Reboto, V.; Reboto V Fau - Molina-
1005 Martinez, I. T.; Molina-Martinez It Fau - Rodriguez-Cabello, J. C.; Rodriguez-Cabello, J. C., Self-assembled
1006 particles of an elastin-like polymer as vehicles for controlled drug release. *J Control Release* **2005**, *102*(1),
1007 (0168-3659 (Print)).

1008 79. Bellingham, C. M.; Lillie, M. A.; Gosline, J. M.; Wright, G. M.; Starcher, B. C.; Bailey, A. J.; Woodhouse, K.
1009 A.; Keeley, F. W., Recombinant human elastin polypeptides self-assemble into biomaterials with elastin-
1010 like properties. *Biopolymers* **2003**, *70*, (4), 445-455.

1011 80. Reguera, J.; Fahmi, A.; Moriarty, P.; Girotti, A.; Rodríguez-Cabello, J. C., Nanopore Formation by Self-
1012 Assembly of the Model Genetically Engineered Elastin-like Polymer [(VPGVG)2(VPGEG)(VPGVG)2]15.
1013 *Journal of the American Chemical Society* **2004**, *126*, (41), 13212-13213.

1014 81. Hecht Stacie, E.; Niehoff Raymond, L.; Narasimhan, K.; Neal Charles, W.; Forshey Paul, A.; Phan Dean, V.;
1015 Brooker Anju Deepali, M.; Combs Katherine, H. Extracting biopolymers from a biomass using ionic liquids.
1016 2010.

1017 82. Zhang, Y.; Li, W.-Y.; Lan, R.; Wang, J.-Y., Quality Monitoring of Porous Zein Scaffolds: A Novel
1018 Biomaterial. *Engineering* **2017**, *3*, (1), 130-135.

1019 83. Zein: a potential biomaterial for tissue engineering: Tissue engineering. *Materials Today* **2004**, *7*, (7-8), 24-
1020 24.

1021 84. Lee, S.; Alwahab, N. S. A.; Moazzam, Z. M., Zein-based oral drug delivery system targeting activated
1022 macrophages. *International Journal of Pharmaceutics* **2013**, *454*, (1), 388-393.

1023 85. Shi, K.; Huang, Y.; Yu, H.; Lee, T.-C.; Huang, Q., Reducing the brittleness of zein films through chemical
1024 modification. *Journal of agricultural and food chemistry* **2011**, *59*, (1), 56.

1025 86. Biswas, A.; Shogren, R. L.; Stevenson, D. G.; Willett, J. L.; Bhowmik, P. K., Ionic liquids as solvents for
1026 biopolymers: Acylation of starch and zein protein. *Carbohydrate Polymers* **2006**, *66*, (4), 546-550.

1027 87. Choi, H.-M.; Kwon, I., Dissolution of Zein Using Protic Ionic Liquids: N-(2-Hydroxyethyl) Ammonium
1028 Formate and N-(2-Hydroxyethyl) Ammonium Acetate. *Industrial & Engineering Chemistry Research* **2011**,
1029 *50*, (4), 2452-2454.

1030 88. Desai, H. E., Synthesis and Structural Characterization of Reflectin Proteins. In North Georgia, C.; State
1031 Univ, D., Eds. 2012.

1032 89. Tao, A. R.; Demartini, D. G.; Izumi, M.; Sweeney, A. M.; Holt, A. L.; Morse, D. E., The role of protein
1033 assembly in dynamically tunable bio-optical tissues. *Biomaterials* **2010**, *31*, (5), 793-801.

1034 90. Arulmoli, J., Scaffolds for Neural Stem Cell Tissue Engineering. **2016**.

1035 91. Kramer, R. M.; Crookes-Goodson, W. J.; Naik, R. R., The self-organizing properties of squid reflectin
1036 protein. *Nature Materials* **2007**, *6*, (7), 533-538.

1037 92. Levenson, R.; Demartini, D. G.; Morse, D. E., Molecular mechanism of reflectin's tunable biophotonic
1038 control: Opportunities and limitations for new optoelectronics. *APL Materials* **2017**, *5*, (10).

1039 93. Levenson, R.; Bracken, C.; Sharma, C.; Santos, J.; Arata, C.; Malady, B.; Morse, D. E., Calibration between
1040 trigger and color: Neutralization of a genetically encoded coulombic switch and dynamic arrest precisely
1041 tune reflectin assembly. *The Journal of biological chemistry* **2019**, *294*, (45), 16804-16815.

1042 94. Thomas, M. S.; Koshy, R. R.; Mary, S. K.; Thomas, S.; Pothan, L. A., *Starch, Chitin and Chitosan Based*
1043 *Composites and Nanocomposites*. Springer International Publishing: 2018.

1044 95. Liu, H.; Xie, F.; Yu, L.; Chen, L.; Li, L., Thermal processing of starch-based polymers. *Progress in Polymer*
1045 *Science* **2009**, *34*, (12), 1348-1368.

1046 96. Kadokawa, J.-I.; Murakami, M.-A.; Takegawa, A.; Kaneko, Y., Preparation of cellulose-starch composite
1047 gel and fibrous material from a mixture of the polysaccharides in ionic liquid. *Carbohydrate Polymers* **2009**,
1048 *75*, (1), 180-183.

1049 97. Carreño, N. L. V., *Advances in Nanostructured Cellulose-based Biomaterials*. 1st ed. 2017. ed.; Springer
1050 International Publishing: Cham, 2017.

1051 98. Freire, M. G.; Teles, A. R. R.; Ferreira, R. A. S.; Carlos, L. D.; Lopes-da-Silva, J. A.; Coutinho, J. A. P.,
1052 Electrospun nanosized cellulose fibers using ionic liquids at room temperature. *Green Chemistry* **2011**, *13*,
1053 (11), 3173-3180.

1054 99. Xu, H.; Bronner, T.; Yamamoto, M.; Yamane, H., Regeneration of cellulose dissolved in ionic liquid using
1055 laser-heated melt-electrospinning. *Carbohydrate Polymers* **2018**, *201*, 182-188.

1056 100. Hermanutz, F.; Vocht, M. P.; Panzier, N.; Buchmeiser, M. R., Processing of Cellulose Using Ionic Liquids.
1057 *Macromolecular Materials and Engineering* **2019**, *304*, (2), 1800450.

1058 101. Liu, Y.; Meyer, A. S.; Nie, Y.; Zhang, S.; Thomsen, K., Low energy recycling of ionic liquids via freeze
1059 crystallization during cellulose spinning. *Green Chemistry* **2018**, *20*, (2), 493-501.

1060 102. Defrates, K.; Markiewicz, T.; Callaway, K.; Xue, Y.; Stanton, J.; Salas-de La Cruz, D.; Hu, X., Structure-
1061 property relationships of Thai silk-microcrystalline cellulose biocomposite materials fabricated from ionic
1062 liquid. *International Journal of Biological Macromolecules* **2017**, *104*, (Pt A), 919-928.

1063 103. Kaya, M.; Mujtaba, M.; Ehrlich, H.; Salaberria, A. M.; Baran, T.; Amemiya, C. T.; Galli, R.; Akyuz, L.; Sargin,
1064 I.; Labidi, J., On chemistry of γ -chitin. *Carbohydrate Polymers* **2017**, *176*, 177-186.

1065 104. Levengood, S. K. L.; Zhang, M., Chitosan-based scaffolds for bone tissue engineering. *Journal of Materials
1066 Chemistry B* **2014**, *2*, (21), 3161-3184.

1067 105. Barber, P. S.; Kelley, S. P.; Griggs, C. S.; Wallace, S.; Rogers, R. D., Surface modification of ionic liquid-spun
1068 chitin fibers for the extraction of uranium from seawater: seeking the strength of chitin and the chemical
1069 functionality of chitosan. *Green Chemistry* **2014**, *16*, (4), 1828-1836.

1070 106. Jaworska, M. M.; Stępiak, I.; Galiński, M.; Kasprzak, D.; Biniaś, D.; Górkak, A., Modification of chitin
1071 structure with tailored ionic liquids. *Carbohydrate Polymers* **2018**, *202*, 397-403.

1072 107. Shigemasa, Y.; Matsuura, H.; Sashiwa, H.; Saimoto, H., Evaluation of different absorbance ratios from
1073 infrared spectroscopy for analyzing the degree of deacetylation in chitin. *International Journal of Biological
1074 Macromolecules* **1996**, *18*, (3), 237-242.

1075 108. *Alginates and Their Biomedical Applications*. 1st ed. 2018. ed.; Springer Singapore: Singapore, 2018.

1076 109. Moradali, M. F.; Donati, I.; Sims, I. M.; Ghods, S.; Rehm, B. H. A., Alginate Polymerization and Modification
1077 Are Linked in <span class="named-content genus-species" id="named-content-
1078 1">Pseudomonas aeruginosa. *mBio* **2015**, *6*, (3), e00453-15.

1079 110. Douthit, S. A.; Dlakic, M.; Ohman, D. E.; Franklin, M. J., Epimerase Active Domain of
1080 Pseudomonas aeruginosa AlgG, a Protein That Contains a Right-Handed β -Helix.
1081 *Journal of Bacteriology* **2005**, *187*, (13), 4573.

1082 111. Mørch, Y. A.; Donati, I.; Strand, B. L., Effect of Ca^{2+} , Ba^{2+} , and Sr^{2+} on Alginate Microbeads.
1083 *Biomacromolecules* **2006**, *7*, (5), 1471-1480.

1084 112. Ouwerx, C.; Velings, N.; Mestdagh, M. M.; Axelos, M. A. V., Physico-chemical properties and rheology of
1085 alginate gel beads formed with various divalent cations. *Polymer Gels and Networks* **1998**, *6*, (5), 393-408.

1086 113. Braccini, I.; Pérez, S., Molecular Basis of Ca^{2+} -Induced Gelation in Alginates and Pectins: The Egg-Box
1087 Model Revisited. *Biomacromolecules* **2001**, *2*, (4), 1089-1096.

1088 114. Sikorski, P.; Mo, F.; Skjåk-Bræk, G.; Stokke, B. T., Evidence for Egg-Box-Compatible Interactions in
1089 Calcium-Alginate Gels from Fiber X-ray Diffraction. *Biomacromolecules* **2007**, *8*, (7), 2098-2103.

1090 115. Skjåk-Bræk, G.; Paoletti, S.; Gianferrara, T., Selective acetylation of mannuronic acid residues in calcium
1091 alginate gels. *Carbohydrate Research* **1989**, *185*, 119-129.

1092 116. Straatmann, A.; Windhues, T.; Borchard, W. In *Effects of acetylation on thermodynamic properties of seaweed
1093 alginate in sodium chloride solutions*, Analytical Ultracentrifugation VII, Berlin, Heidelberg, 2004//, 2004;
1094 Lechner, M. D.; Börger, L., Eds. Springer Berlin Heidelberg: Berlin, Heidelberg, 2004; pp 26-30.

1095 117. Delben, F.; Cesaro, Á.; Paoletti, S.; Crescenzi, V., Monomer composition and acetyl content as main
1096 determinants of the ionization behavior of alginates. *Carbohydrate Research* **1982**, *100*, (1), C46-C50.

1097 118. Cook, W., Alginate dental impression materials: chemistry, structure, and properties. *J Biomed Mater Res*
1098 1986, 20, (0021-9304 (Print)).

1099 119. Craig, R. G., Review of Dental Impression Materials. *Advances in Dental Research* 1988, 2, (1), 51-64.

1100 120. Groves, A. R.; Lawrence, J. C., Alginate dressing as a donor site haemostat. *Ann R Coll Surg Engl* 1986, 68,
1101 (1), 27-28.

1102 121. Barnett, S. E.; Varley, S. J., The effects of calcium alginate on wound healing. *Ann R Coll Surg Engl* 1987, 69,
1103 (4), 153-155.

1104 122. Hrynyk, M.; Martins-Green, M.; Barron, A. E.; Neufeld, R. J., Alginate-PEG sponge architecture and role in
1105 the design of insulin release dressings. *Biomacromolecules* 2012, 13, (5), 1478-1485.

1106 123. Barbetta, A.; Barigelli, E.; Dentini, M., Porous Alginate Hydrogels: Synthetic Methods for Tailoring the
1107 Porous Texture. *Biomacromolecules* 2009, 10, (8), 2328-2337.

1108 124. Andersen, T.; Melvik, J. E.; Gåserød, O.; Alsberg, E.; Christensen, B. E., Ionically Gelled Alginate Foams:
1109 Physical Properties Controlled by Operational and Macromolecular Parameters. *Biomacromolecules* 2012,
1110 13, (11), 3703-3710.

1111 125. Shin, S.-J.; Park, J.-Y.; Lee, J.-Y.; Park, H.; Park, Y.-D.; Lee, K.-B.; Whang, C.-M.; Lee, S.-H., "On the Fly"
1112 Continuous Generation of Alginate Fibers Using a Microfluidic Device. *Langmuir* 2007, 23, (17), 9104-9108.

1113 126. Daemi, H.; Barikani, M.; Barmar, M., Highly stretchable nanoalginate based polyurethane elastomers.
1114 *Carbohydrate Polymers* 2013, 95, (2), 630-636.

1115 127. Senuma, Y.; Lowe, C.; Zweifel, Y.; Hilborn, J. G.; Marison, I., Alginate hydrogel microspheres and
1116 microcapsules prepared by spinning disk atomization. *Biotechnology and Bioengineering* 2000, 67, (5), 616-
1117 622.

1118 128. Bodmeier, R.; Chen, H.; Paeratakul, O., A Novel Approach to the Oral Delivery of Micro- or Nanoparticles.
1119 *Pharmaceutical Research* 1989, 6, (5), 413-417.

1120 129. Iqbal, B.; Sarfaraz, Z.; Muhammad, N.; Ahmad, P.; Iqbal, J.; Khan, Z. U. H.; Gonfa, G.; Iqbal, F.; Jamal, A.;
1121 Rahim, A., Ionic liquid as a potential solvent for preparation of collagen-alginate-hydroxyapatite beads as
1122 bone filler. *Journal of biomaterials science. Polymer edition* 2018, 29, (10), 1168-1184.

1123 130. Rufato, K. B.; Almeida, V. C.; Kipper, M. J.; Rubira, A. F.; Martins, A. F.; Muniz, E. C., Polysaccharide-based
1124 adsorbents prepared in ionic liquid with high performance for removing Pb(II) from aqueous systems.
1125 *Carbohydrate Polymers* 2019, 215, 272-279.

1126 131. Shin, Y. M.; Hohman, M. M.; Brenner, M. P.; Rutledge, G. C., Experimental characterization of
1127 electrospinning: the electrically forced jet and instabilities. *Polymer* 2001, 42, (25), 09955-09967.

1128 132. Lyons, J.; Li, C.; Ko, F., Melt-electrospinning part I: processing parameters and geometric properties.
1129 *Polymer* 2004, 45, (22), 7597-7603.

1130 133. Chronakis, I. S., Novel nanocomposites and nanoceramics based on polymer nanofibers using
1131 electrospinning process—A review. *Journal of Materials Processing Technology* 2005, 167, (2), 283-293.

1132 134. Green, M. D.; Long, T. E., Designing Imidazole-Based Ionic Liquids and Ionic Liquid Monomers for
1133 Emerging Technologies. *Polymer Reviews* 2009, 49, (4), 291-314.

1134 135. Xu, J.-M.; Wu, W.-B.; Qian, C.; Liu, B.-K.; Lin, X.-F., A novel and highly efficient protocol for Markovnikov's
1135 addition using ionic liquid as catalytic green solvent. *Tetrahedron Letters* 2006, 47, (10), 1555-1558.

1136 136. Kong, C. S.; Yoo, W. S.; Jo, N. G.; Kim, H. S., Electrospinning Mechanism for Producing Nanoscale Polymer
1137 Fibers. *Journal of Macromolecular Science, Part B* 2010, 49, (1), 122-131.

1138 137. Kulpinski, P., Cellulose nanofibers prepared by the N-methylmorpholine-N-oxide method. *Journal of
1139 Applied Polymer Science* 2005, 98, (4), 1855-1859.

1140 138. Rosenau, T.; Potthast, A.; Adorjan, I.; Hofinger, A.; Sixta, H.; Firgo, H.; Kosma, P., Cellulose solutions in
1141 N-methylmorpholine-N-oxide (NMMO) – degradation processes and stabilizers. *Cellulose* **2002**, *9*, (3), 283-
1142 291.

1143 139. de Vasconcelos, C. L.; Bezerril, P. M.; Pereira, M. R.; Ginani, M. F.; Fonseca, J. L. C., Viscosity-temperature
1144 behavior of chitin solutions using lithium chloride/DMA as solvent. *Carbohydrate Research* **2011**, *346*, (5),
1145 614-618.

1146 140. Kurland, N. E.; Dey, T.; Wang, C.; Kundu, S. C.; Yadavalli, V. K., Silk Protein Lithography as a Route to
1147 Fabricate Sericin Microarchitectures. *Advanced Materials* **2014**, *26*, (26), 4431-4437.

1148 141. Pal, R. K.; Kurland, N. E.; Wang, C.; Kundu, S. C.; Yadavalli, V. K., Biopatterning of Silk Proteins for Soft
1149 Micro-optics. *ACS Applied Materials & Interfaces* **2015**, *7*, (16), 8809-8816.

1150 142. Pal, R. K.; Farghaly, A. A.; Wang, C.; Collinson, M. M.; Kundu, S. C.; Yadavalli, V. K., Conducting polymer-
1151 silk biocomposites for flexible and biodegradable electrochemical sensors. *Biosensors and Bioelectronics* **2016**,
1152 81, 294-302.

1153 143. Yao, C.; Li, X.; Song, T.; Li, Y.; Pu, Y., Biodegradable nanofibrous membrane of zein/silk fibroin by
1154 electrospinning. *Polymer International* **2009**, *58*, (4), 396-402.

1155 144. Wang, F.; Yu, H.-y.; Gu, Z.-G.; Si, L.; Liu, Q.-c.; Hu, X., Impact of calcium chloride concentration on
1156 structure and thermal property of Thai silk fibroin films. *Journal of Thermal Analysis and Calorimetry* **2017**,
1157 130, (2), 851-859.

1158 145. Gubitosi, M.; Duarte, H.; Gentile, L.; Olsson, U.; Medronho, B., On cellulose dissolution and aggregation
1159 in aqueous tetrabutylammonium hydroxide. *Biomacromolecules* **2016**, *17*, (9), 2873-2881.

1160 146. Behrens, M. A.; Holdaway, J. A.; Nosrati, P.; Olsson, U., On the dissolution state of cellulose in aqueous
1161 tetrabutylammonium hydroxide solutions. *RSC Advances* **2016**, *6*, (36), 30199-30204.

1162 147. Medronho, B.; Filipe, A.; Napso, S.; Khalfin, R. L.; Pereira, R. F. P.; de Zea Bermudez, V.; Romano, A.;
1163 Cohen, Y., Silk Fibroin Dissolution in Tetrabutylammonium Hydroxide Aqueous Solution. *Biomacromolecules* **2019**, *20*, (11), 4107-4116.

1164 148. Sang, Q.; Williams, G. R.; Wu, H.; Liu, K.; Li, H.; Zhu, L.-M., Electrospun gelatin/sodium bicarbonate and
1165 poly(lactide-co-ε-caprolactone)/sodium bicarbonate nanofibers as drug delivery systems. *Materials Science
1166 and Engineering: C* **2017**, *81*, 359-365.

1167 149. Anton, F. Process and apparatus for preparing artificial threads. 1930.

1168 150. Abdul Khalil, H. P. S.; Davoudpour, Y.; Bhat, A. H.; Rosamah, E.; Tahir, P. M., Electrospun Cellulose
1169 Composite Nanofibers. In *Handbook of Polymer Nanocomposites. Processing, Performance and Application: Volume C: Polymer Nanocomposites of Cellulose Nanoparticles*, Pandey, J. K.; Takagi, H.; Nakagaito, A. N.; Kim,
1170 H.-J., Eds. Springer Berlin Heidelberg: Berlin, Heidelberg, 2015; pp 191-227.

1171 151. Baji, A.; Mai, Y.-W.; Wong, S.-C.; Abtahi, M.; Chen, P., Electrospinning of polymer nanofibers: Effects on
1172 oriented morphology, structures and tensile properties. *Composites Science and Technology* **2010**, *70*, (5), 703-
1173 718.

1174 152. Gupta, P.; Wilkes, G. L., Some investigations on the fiber formation by utilizing a side-by-side bicomponent
1175 electrospinning approach. *Polymer* **2003**, *44*, (20), 6353-6359.

1176 153. Kenawy, E.-R.; Abdel-Hay, F. I.; El-Newehy, M. H.; Wnek, G. E., Processing of polymer nanofibers through
1177 electrospinning as drug delivery systems. *Materials Chemistry and Physics* **2009**, *113*, (1), 296-302.

1178 154. Hu, X.; Liu, S.; Zhou, G.; Huang, Y.; Xie, Z.; Jing, X., Electrospinning of polymeric nanofibers for drug
1179 delivery applications. *Journal of Controlled Release* **2014**, *185*, 12-21.

1180

1181

1182 155. Shamshina, J. L.; Zavgorodnya, O.; Bonner, J. R.; Gurau, G.; Di Nardo, T.; Rogers, R. D., "Practical"
1183 Electrospinning of Biopolymers in Ionic Liquids. *ChemSusChem* **2017**, *10*, (1), 106-111.

1184 156. Pelipenko, J.; Kristl, J.; Janković, B.; Baumgartner, S.; Kocbek, P., The impact of relative humidity during
1185 electrospinning on the morphology and mechanical properties of nanofibers. *International Journal of*
1186 *Pharmaceutics* **2013**, *456*, (1), 125-134.

1187 157. Cramariuc, B.; Cramariuc, R.; Scarlet, R.; Manea, L. R.; Lupu, I. G.; Cramariuc, O., Fiber diameter in
1188 electrospinning process. *Journal of Electrostatics* **2013**, *71*, (3), 189-198.

1189 158. Bae, H.-S.; Haider, A.; Selim, K. M. K.; Kang, D.-Y.; Kim, E.-J.; Kang, I.-K., Fabrication of highly porous
1190 PMMA electrospun fibers and their application in the removal of phenol and iodine. *Journal of Polymer*
1191 *Research* **2013**, *20*, (7), 158.

1192 159. Yudin, V. E.; Dobrovolskaya, I. P.; Neelov, I. M.; Dresvyanina, E. N.; Popryadukhin, P. V.; Ivan'kova, E.
1193 M.; Elokhovskii, V. Y.; Kasatkin, I. A.; Okrugin, B. M.; Morganti, P., Wet spinning of fibers made of chitosan
1194 and chitin nanofibrils. *Carbohydrate Polymers* **2014**, *108*, 176-182.

1195 160. Lucia, L.; Ayoub, A., *Polysaccharide-based Fibers and Composites: Chemical and Engineering Fundamentals and*
1196 *Industrial Applications*. Springer International Publishing: 2017.

1197 161. DeFrates, K. G.; Moore, R.; Borgesi, J.; Lin, G.; Mulderig, T.; Beachley, V.; Hu, X., Protein-Based Fiber
1198 Materials in Medicine: A Review. *Nanomaterials (Basel)* **2018**, *8*, (7), 457.

1199 162. Lee, K.; Baek, D.; Ki, C.; Park, Y. H., Preparation and characterization of wet spun silk fibroin/poly(vinyl
1200 alcohol) blend filaments. *International journal of biological macromolecules* **2007**, *41*, 168-72.

1201 163. Nayak, R.; Padhye, R.; Kyratzis, I. L.; Truong, Y. B.; Arnold, L., Recent advances in nanofibre fabrication
1202 techniques. *Textile Research Journal* **2011**, *82*, (2), 129-147.

1203 164. Grimmelmann, N.; Grothe, T.; Homburg, S. V.; Ehrmann, A., Electropinning and stabilization of chitosan
1204 nanofiber mats. In Institute of Physics Publishing: 2017; Vol. 254.

1205 165. Stanton, J.; Xue, Y.; Waters, J. C.; Lewis, A.; Cowan, D.; Hu, X.; la Cruz, D. S.-d., Structure–property
1206 relationships of blended polysaccharide and protein biomaterials in ionic liquid. *Cellulose* **2017**, *24*, (4),
1207 1775-1789.

1208 166. Love, S. A.; Popov, E.; Rybacki, K.; Hu, X.; Salas-de la Cruz, D., Facile treatment to fine-tune cellulose
1209 crystals in cellulose-silk biocomposites through hydrogen peroxide. *International Journal of Biological*
1210 *Macromolecules* **2020**, *147*, 569-575.

1211 167. Pereira, R. F. P.; Brito-Pereira, R.; Goncalves, R.; Silva, M. P.; Costa, C. M.; Silva, M. M.; de Zea Bermudez,
1212 V.; Lanceros-Mendez, S., Silk Fibroin Separators: A Step Toward Lithium-Ion Batteries with Enhanced
1213 Sustainability. *ACS Appl Mater Interfaces* **2018**, *10*, (6), 5385-5394.

1214 168. Haverhals, L. M.; Sulpizio, H. M.; Fayos, Z. A.; Trulove, M. A.; Reichert, W. M.; Foley, M. P.; De Long, H.
1215 C.; Trulove, P. C., Process variables that control natural fiber welding: time, temperature, and amount of
1216 ionic liquid. *Cellulose* **2012**, *19*, (1), 13-22.

1217 169. Ebner, G.; Schiehser, S.; Potthast, A.; Rosenau, T., Side reaction of cellulose with common 1-alkyl-3-
1218 methylimidazolium-based ionic liquids. *Tetrahedron Letters* **2008**, *49*, (51), 7322-7324.

1219 170. Wu, J.; Zhang, J.; Zhang, H.; He, J.; Ren, Q.; Guo, M., Homogeneous Acetylation of Cellulose in a New Ionic
1220 Liquid. *Biomacromolecules* **2004**, *5*, (2), 266-268.

1221 171. Cruz, D. S.-d. I. Morphology and ionic conductivity of polymerized ionic liquids. University of
1222 Pennsylvania, UMI Dissertation Publishing, Ann Arbor, MI, 2011.

1223 172. Klein, R. J.; Zhang, S.; Dou, S.; Jones, B. H.; Colby, R. H.; Runt, J., Modeling electrode polarization in
1224 dielectric spectroscopy: Ion mobility and mobile ion concentration of single-ion polymer electrolytes. *The
1225 Journal of Chemical Physics* **2006**, *124*, (14), 144903.

1226 173. Salas-de La Cruz, D., Morphology and ionic conductivity of polymerized ionic liquids. In Winey, K. I., Ed.
1227 ProQuest Dissertations Publishing: 2011.

1228 174. Lovrić, M., Solid state electrochemistry (1995) Peter G. Bruce (ed). *Journal of Solid State Electrochemistry* **1997**,
1229 1, (1), 116-116.

1230 175. Chen, H.; Choi, J.-H.; Salas-de la Cruz, D.; Winey, K. I.; Elabd, Y. A., Polymerized Ionic Liquids: The Effect
1231 of Random Copolymer Composition on Ion Conduction. *Macromolecules* **2009**, *42*, (13), 4809-4816.

1232 176. Shin, E. J.; Choi, S. M.; Singh, D.; Zo, S. M.; Lee, Y. H.; Kim, J. H.; Han, S. S., Fabrication of cellulose-based
1233 scaffold with microarchitecture using a leaching technique for biomedical applications. *Cellulose* **2014**, *21*,
1234 (5), 3515-3525.

1235 177. Li, L.; Meng, L.; Zhang, X.; Fu, C.; Lu, Q., The ionic liquid-associated synthesis of a cellulose/SWCNT
1236 complex and its remarkable biocompatibility. *Journal of Materials Chemistry* **2009**, *19*, (22), 3612-3617.

1237 178. Liu, Y.; Nguyen, A.; Allen, A.; Zoldan, J.; Huang, Y.; Chen, J. Y., Regenerated cellulose micro-nano fiber
1238 matrices for transdermal drug release. *Materials Science & Engineering C* **2017**, *74*, 485-492.

1239 179. Ma, H.; Hsiao, B. S.; Chu, B., Thin-film nanofibrous composite membranes containing cellulose or chitin
1240 barrier layers fabricated by ionic liquids. *Polymer* **2011**, *52*, (12), 2594-2599.

1241 180. Heinze, T.; Liebert, T., Unconventional methods in cellulose functionalization. *Progress in Polymer Science*
1242 **2001**, *26*, (9), 1689-1762.

1243 181. Moniruzzaman, M.; Ono, T., Separation and characterization of cellulose fibers from cypress wood treated
1244 with ionic liquid prior to laccase treatment. *Bioresource Technology* **2013**, *127*, 132-137.

1245 182. Haerens, K.; Van Deuren, S.; Matthijs, E.; Van der Bruggen, B., Challenges for recycling ionic liquids by
1246 using pressure driven membrane processes. *Green Chemistry* **2010**, *12*, (12), 2182-2188.

1247 183. Yu, X.; Bao, X.; Zhou, C.; Zhang, L.; Yagoub, A. E.-G. A.; Yang, H.; Ma, H., Ultrasound-ionic liquid
1248 enhanced enzymatic and acid hydrolysis of biomass cellulose. *Ultrasonics Sonochemistry* **2018**, *41*, 410-418.

1249 184. Dias, J. C.; Lopes, A. C.; Magalhães, B.; Botelho, G.; Silva, M. M.; Esperança, J. M. S. S.; Lanceros-Mendez,
1250 S., High performance electromechanical actuators based on ionic liquid/poly(vinylidene fluoride). *Polymer
1251 Testing* **2015**, *48*, 199-205.

1252 185. Kim, O.; Shin, T. J.; Park, M. J., Fast low-voltage electroactive actuators using nanostructured polymer
1253 electrolytes. *Nature Communications* **2013**, *4*, (1), 2208.

1254



© 2020 by the authors. Submitted for possible open access publication under the terms
and conditions of the Creative Commons Attribution (CC BY) license
(<http://creativecommons.org/licenses/by/4.0/>).